

## JGR Biogeosciences

## RESEARCH ARTICLE

10.1029/2019JG005113

## Key Points:

- Fluorescence imaging facilitates the understanding of biological processes
- Fluorescent and fluorogenic probes can be applied to foraminifera
- Fluorescence-based methods are powerful techniques to visualize certain ultrastructural organization of foraminiferal cells

## Supporting Information:

- Supporting Information S1
- Table S1
- Figure S1
- Figure S2
- Figure S3
- Movie S1

## Correspondence to:

F. Frontalini,  
fabrizio.frontalini@uniurb.it

## Citation:

Frontalini, F., Losada, M. T., Toyofuku, T., Tyszka, J., Goleń, J., de Nooijer, L., et al. (2019). Foraminiferal ultrastructure: A perspective from fluorescent and fluorogenic probes. *Journal of Geophysical Research: Biogeosciences*, 124, 2823–2850. <https://doi.org/10.1029/2019JG005113>

Received 26 FEB 2019

Accepted 26 JUL 2019

Accepted article online 12 AUG 2019

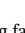

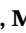
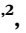

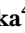










Published online 9 SEP 2019

Corrected 22 OCT 2019

This article was corrected on 22 OCT 2019. See the end of the full text for details.

©2019. American Geophysical Union.  
All Rights Reserved.

## Foraminiferal Ultrastructure: A perspective From Fluorescent and Fluorogenic Probes

F. Frontalini<sup>1</sup> , M. T. Losada<sup>1,2</sup>, T. Toyofuku<sup>3</sup> , J. Tyszka<sup>4</sup> , J. Goleń<sup>4</sup> , L. de Nooijer<sup>5</sup> , B. Canonico<sup>6</sup> , E. Cesarini<sup>6</sup> , Y. Nagai<sup>3</sup> , U. Bickmeyer<sup>7</sup> , T. Ikuta<sup>8</sup> , R. Tsubaki<sup>3</sup>, C. Besteiro Rodriguez<sup>2</sup> , E. Al-Enezi<sup>9</sup> , S. Papa<sup>6</sup> , R. Coccioni<sup>1</sup> , J. Bijma<sup>7</sup> , and J. M. Bernhard<sup>10</sup> 

<sup>1</sup>Department of Pure and Applied Sciences, University of Urbino, Urbino, Italy, <sup>2</sup>Departamento de Zooloxía e Antropoloxía Física, Universidade de Santiago de Compostela, Lugo, Spain, <sup>3</sup>Institute for Extra-cutting-edge Science and Technology Avant-garde Research (X-star), Japan Agency for Marine-Earth Science and Technology, Yokosuka, Japan, <sup>4</sup>Institute of Geological Sciences, Polish Academy of Sciences, Kraków, Poland, <sup>5</sup>Royal Netherlands Institute for Sea Research, Horntje, Netherlands, <sup>6</sup>Department of Biomolecular Sciences, University of Urbino, Urbino, Italy, <sup>7</sup>Alfred-Wegener-Institut Helmholtz-Zentrum für Polar- und Meeresforschung, Bremerhaven, Germany, <sup>8</sup>Research Institute for Global Change, Japan Agency for Marine-Earth Science and Technology, Yokosuka, Japan, <sup>9</sup>Kuwait Institute for Scientific Research, Safat, Kuwait, <sup>10</sup>Geology and Geophysics Department, Woods Hole Oceanographic Institution, Woods Hole, MA, USA

**Abstract** Microscopy techniques have been widely applied to observe cellular ultrastructure. Most of these techniques, such as transmission electron microscopy, produce high-resolution images, but they may require extensive preparation, hampering their application for in vivo examination. Other approaches, such as fluorescent and fluorogenic probes, can be applied not only to fixed specimens but also to living cells when the probes are nontoxic. Fluorescence-based methods, which are generally relatively easy to use, allow visual and (semi)quantitative studies of the ultrastructural organization and processes of the cell under natural as well as manipulated conditions. To date, there are relatively few published studies on the nearly ubiquitous marine protistan group Foraminifera that have used fluorescent and fluorogenic probes, despite their huge potential. The aim of the present contribution is to document the feasible application of a wide array of these probes to foraminiferal biology. More specifically, we applied fluorescence-based probes to study esterase activity, cell viability, calcium signaling, pH variation, reactive oxygen species, neutral and polar lipids, lipid droplets, cytoskeleton structures, Golgi complex, acidic vesicles, nuclei, and mitochondria in selected foraminiferal species.

## 1. Introduction

Foraminifera are ubiquitous, mostly marine, single-celled eukaryotes, with their cell body commonly enclosed in test (e.g., Anderson & Lee, 1991). The characteristics that distinguish foraminifera from most other protists are their granuloreticulopodia (Goldstein, 1999), which are fine, thread-like pseudopodia with a granular appearance that protrude through apertures to stream and anastomose in a web-like halo (Jahn & Rinaldi, 1959; Travis & Allen, 1981; Travis & Bowser, 1986a, 1986b, 1991). As in other eukaryotic cells, membrane-enclosed compartments like nuclei, ribosomes, endoplasmic reticula, Golgi complexes, mitochondria, lysosomes, degradation vacuoles, residual bodies, peroxisomes, fibrillar vesicles, and electron-opaque bodies can be distinguished within foraminiferal cytoplasm (LeKieffre et al., 2018). Lipid droplets and pigment inclusions are membrane-enclosed compartments that can also be present in the cytoplasm (Debenay et al., 1996).

Over the last four decades, foraminifera have been used as environmental proxies (i.e., Armynot du Châtelet & Debenay, 2010; Desandier et al., 2015; Frontalini & Coccioni, 2011). Foraminifera react to environmental changes by varying assemblages' composition and parameters and, at the species level, by modifying the test, reproductive capacity, and cellular ultrastructure (e.g., Frontalini & Coccioni, 2008; Yanko et al., 1999). To date, many studies have focused on assemblage and morphological responses to environmental change. Our knowledge of the foraminiferal response to unfavorable environmental conditions remains far from complete. Moreover, very little is known about the cytological alterations of these organisms under stressful conditions (e.g., Frontalini et al., 2018; Koho et al., 2018; Nomaki et al., 2016).

Most cytological studies on foraminifera have been performed via microscopy techniques by observing the ultrastructure of the foraminiferal cell (e.g., Anderson & Lee, 1991; Jahn & Rinaldi, 1959; Ohno et al.,

2016; Travis & Allen, 1981; Travis & Bowser, 1991; Tyszka et al., 2019) and have aimed to link the foraminiferal ultrastructure to physiological processes and environmental conditions (e.g., Bernhard et al., 2010; Bernhard & Bowser, 1999; Bernhard & Bowser, 2008; Frontalini et al., 2018; Goldstein & Richardson, 2018; Jauffrais et al., 2018; Koho et al., 2018). To study the adaptations of foraminiferal ultrastructure to habitat, researchers have developed different transmission electron microscopy-coupled (TEM-coupled) techniques (reviewed in Nomaki et al., 2018). Even though TEM-based techniques allow scientists to obtain high-resolution images, such methods commonly involve a lengthy series of preparation steps that can hamper their application for other purposes and excludes *in vivo* assessments.

To help fill the knowledge gap regarding metabolic processes and ultrastructural dynamics in general, fluorescent and fluorogenic probes were developed to be applied to chemically fixed specimens as well as living ones (see Le Droumaguet et al., 2010; Shieh et al., 2012, for reviews). Fluorogenic probes comprise nonfluorescent membrane-permeant chemical compounds that, once passing the cell membrane, are activated by an enzyme; this modification creates fluorescence if excited with the correct wavelength (e.g., Shieh et al., 2012). In the case of fluorescent probes, they do not need to be modified by enzymes, as they fluoresce when they bind to the structural target (e.g., Bernhard et al., 1995; de Nooijer, Toyofuku, et al., 2009). Fluorescence-based methods allow visual and quantitative studies of the structural and chemical organization of the cell, enabling assessments of cellular ultrastructural dynamics under natural conditions as well as their response to changes in the environment (Frontalini et al., 2015; Yanko et al., 1999). Moreover, the application of multicolor fluorescence labeling allows simultaneous targeting of different organelles and physiological processes.

This contribution tests the applicability of a wide array of selected fluorescent and fluorogenic probes to selected benthic foraminiferal species.

## 2. State-of-the-Art on Fluorescent and Fluorogenic Probe Use in Foraminifera

Although the number of studies that have been performed on foraminifera with fluorescent and fluorogenic probes is still limited, a wide range of applications using fluorogenic and fluorescent probes is emerging from studies of other organisms (Ainsworth et al., 2008). One of the most widespread uses of fluorogenic probes is the assessment of the viability of foraminifera, as other methods lead to overestimations of living individuals or false positives (e.g., Bernhard, 1988; Bernhard et al., 2006; Murray & Bowser, 2000). Seven fluorogenic probes (*diacetates of fluorescein [FDA]*, *carboxyfluorescein*, *dichlorofluorescein*, and *carboxyeosin*; *AM-esters of bis(carboxyethyl)carboxyfluorescein [BCECF-AM]*, *calcein*, and *calcein blue*) were tested on *Allogromia laticollaris* as possible nonterminal methods to distinguish live from dead foraminifera (Bernhard et al., 1995). Bernhard and Bowser (1996) developed a method based on the *CellTracker<sup>TM</sup> Green CMFDA*, as a vital fluorogenic probe that demonstrates the enzymatic activity, and consequently the vitality of the cell (Hintz et al., 2004; Pucci et al., 2009). Another fluorescent probe-based method for identifying living foraminifera was developed by Borrelli et al. (2011), where *fluorescent in situ hybridization (FISH)* oligonucleotides (EUK 1209R and S17) tagged with the fluorescent probe *Cy<sup>TM</sup>-3* are specific to foraminiferal *ribosomal RNA*. This approach can also be used as an indicator of the cellular metabolic activity.

In order to achieve a more complete understanding of foraminiferal intracellular activities additional fluorogenic probes have been tested and applied. For example, *SlowFade<sup>®</sup>* was used to preserve the autofluorescent signals of plastids in *Elphidium excavatum* (Correia & Lee, 2002). Selectivity of the foraminiferal diet was studied by employing two fluorescent probes (*DAPI* [diamino-2'-phenylindol] and *SYTO<sup>®</sup> 13*) for DNA marking of bacteria, and *Pink SPHERO<sup>TM</sup>* fluorescent polystyrene particles were used as a control to test nonspecific uptake by foraminifera (Langezaal et al., 2005). *DAPI* was used to mark DNA of sequestered chloroplasts in *Haynesina germanica* (Goldstein & Richardson, 2018) and to label foraminiferal nuclei and DNA content in combination with *SlowFade<sup>®</sup> Gold* in *Allogromia laticollaris* (Parfrey & Katz, 2010). Cytoplasmic and pseudopodial observations were performed by Ohno et al. (2016) using Confocal laser scanning microscopy (CLSM) of foraminiferal specimens treated with *Calcein AM*, a molecule that fluoresces when is hydrolysed by intracellular esterases in a living cell.

Foraminiferal tests and especially their geochemistry are basic to paleoenvironmental, paleoceanographic, and paleoclimatic studies; thus, many researchers have focused on foraminiferal calcification using the fluorescent marker *calcein*. *Calcein* (*Bis(N,N-bis(carboxymethyl)aminomethyl)-fluorescein*) is used to label

and distinguish newly grown chambers (Bernhard et al., 2004), allowing the determination of growth and reproduction under controlled laboratory conditions (e.g., Diz et al., 2015; Hintz et al., 2004). Calcein was also used to check the incorporation of trace elements to the new chambers (e.g., de Nooijer et al., 2007; Evans et al., 2018; Kramar et al., 2010; Munsel et al., 2010; Nardelli et al., 2014; Van Dijk, de Nooijer, Wolthers, et al., 2017; van Dijk, de Nooijer, & Reichart, 2017), to assess the role of fluid-phase endocytosis in calcification (Bentov et al., 2009) and in sediment samples to develop a method that can identify the location and timing of calcification (Bernhard et al., 2015). Possible impacts of calcein were evaluated by Bernhard et al. (2004), Dissard et al. (2009), and Kurtarkar et al. (2015), who found that the marker does not affect the survival rate of individuals, incorporation of elements, nor their growth rates.

Other fluorescent probes were also shown to be useful for studying calcification: *Fluo-3AM*, which binds to  $\text{Ca}^{2+}$ , was used to describe calcium intracellular dynamics in living foraminifera (de Nooijer, Langer, et al., 2009; Toyofuku et al., 2008); *FM<sup>®</sup>1-43* was used to label cell membranes to assess their cycling (de Nooijer, Langer, et al., 2009); and *FITC-D (fluorescein isothiocyanate-dextran)*, which is membrane impermeable, was used to assess fluid-phase endocytosis (Bentov et al., 2009; de Nooijer, Langer, et al., 2009; Nehrke et al., 2013). In order to measure intracellular pH, an essential parameter in controlling calcification mechanisms, de Nooijer et al. (2008), de Nooijer, Toyofuku, et al. (2009), and Toyofuku et al. (2017) used the probe *8-Hydroxypyrene-1,3,6-trisulfonic acid (HPTS)*, which has different fluorescence spectra in protonated and deprotonated forms. Bentov et al. (2009) used the membrane impermeable *SNARF<sup>®</sup>-1* to quantify the intracellular change of pH due to seawater endocytosis.

Additional fluorescence-based probes were tested as indicators of cellular changes as a response against xenobiotics. Bresler and Yanko (1995a, 1995b) tested *the reduced nicotinamide adenine nucleotide (NAD-H)* to measure the metabolic state of mitochondria; *acridine orange (AO)* to expose the mucopolysaccharides and to determine both lysosomes and cell viability; neutral red to measure the state of the lysosomes and viability of the cell, *fluorescein* to determine the plasma membrane's permeability and to measure haloperoxidase activity; benzidine to locate the peroxidase activity; and both *FDA (fluorescein diacetate)* and *FDB (fluorescein dibutyrate)* to determine the esterase activity and cell viability. FDA was also used by Bernhard et al. (1995) and Nardelli et al. (2014) to determine foraminiferal esterase activity. More recently, AO and *Nile Red (NR)* in combination with CLSM were used to detect and quantify acidic vesicular organelles and to localize and quantify neutral and polar lipids, respectively (Frontalini et al., 2016). To our knowledge, all publications to date that have used fluorescent and fluorogenic probes directly or indirectly to study benthic foraminifera are reported in Table S1 in the supporting information.

### 3. Materials and Methods

#### 3.1. Site Collection for Living Foraminiferal Specimens

Several species that represent Globothalamea (G) and Tubothalamea (T), that is, two main foraminiferal classes (sensu Pawlowski et al., 2013), namely, *Ammonia parkinsoniana* (G), *Ammonia tepida* (G), *Ammonia beccarii*, *Spirillina vivipara* (T), *Quinqueloculina* sp. (T), *Amphistegina lessonii* (G), *Amphistegina* sp. (G), and *Bolivina variabilis* (G) were used for testing fluorescent and fluorogenic probes as described in this contribution (Table 1). The list of tested probes and, for a matter of completeness, those that have been recently applied to benthic foraminifera (i.e., NR, AO, and SiR-actin) is reported in Table 1. Living specimens of *A. parkinsoniana* were collected off the Monte Conero area (Italy, central Adriatic Sea). Living specimens of *A. tepida* were collected in the lagoon of Bellocchio (NE Italy) and Nojima tidal flat, Tokyo Bay (Japan). Additionally, living specimens of *A. beccarii* (sensu de Nooijer et al., 2008) were taken from salt marsh sediments in Hiragata-Bay (Japan), whereas *S. vivipara* specimens were retrieved from the Enoshia Aquarium, Sagami Bay (Japan). Living specimens of *Quinqueloculina* sp. and *B. variabilis* were collected from marine aquaria in Zoo in Wrocław (Poland). Living specimens of *A. lessonii* were collected from the reef aquarium of the Royal Burgers' Zoo in Arnhem (the Netherlands). Specimens from Wrocław and Arnhem were transferred to the ING PAN Research Centre in Kraków (Poland), where they were separately cultured under controlled conditions (salinity: 33; temperature: 25 °C; day/night light cycle: 12/12 hr, water pump with filter).

**Table 1**  
List of Probes Tested in This Contribution Including Application, Foraminiferal Species, Cell Status, Foraminiferal Specimens (Cultured Versus Natural), and Excitation/Emission Wavelengths

Probe name	Acronym	Application	Foraminiferal species	Number of specimens	Status	Foraminiferal specimens and culture	Excitation/Emission (nm)	Applicability	Pros	Cons
<i>Acridine Orange</i>	AO	Acidic vesicles and Mucopolysaccharides	<i>Ammonia parkinsoniana</i>	100	Living	Natural samples and culture	488/650	Yes	Suitable for live staining, easy staining procedure, membrane permeable	Relatively rapid fading
<i>ActinGreen™</i> 488 Ready Probes®	ActinGreen™	F-Actin	<i>Ammonia parkinsoniana</i> <i>Ammonia tepida</i>	20	Fixed	Natural samples	495/518	Yes	Selective, high-affinity F-actin probe	Cell impermeant, permeabilizer required
<i>BODIPY™</i> TR C5 <i>ceramide</i>	BODIPY™	Golgi complex	<i>Ammonia tepida</i>	20	Fixed and Living	Natural samples	589/617	No	Suitable for live staining and membrane permeable	Long staining procedure
<i>CellHunt™</i> Blue <i>CMHC</i>	CHB	Esterase activity	<i>Ammonia tepida</i>	200	Living	Natural samples and culture	353/466	Yes	Unexpensive and easy procedure	N/A
<i>CellROX™</i> Green	CellROX	ROS	<i>Ammonia tepida</i>	20	Fixed and Living	Natural samples and culture	500/525	Yes	Suitable for live staining, easy staining procedure, membrane permeable	Relatively rapid fading
<i>CellTrace™</i> Calcein <i>Red-Orange</i>	N/A	Cell viability	<i>Quinqueloculina</i> sp. <i>Quinqueloculina</i> sp.	50	Living	Culture	577/590	Yes	Suitable for live staining, easy staining procedure, membrane permeable	Relatively rapid fading
<i>FCS LipidTOX™</i> Green	LipidTOX™	Neutral lipids	<i>Ammonia tepida</i>	20	Fixed	Natural samples	495/525	Yes	Suitable for live staining, easy staining procedure, membrane permeable	N/A
<i>Hoechst 33342</i>	N/A	Nucleic Acids, Nucleus	<i>Ammonia</i> sp. and <i>Spirillina vivipara</i>	20 and 15	Living	Natural samples and culture	350/461	Yes	Suitable for live staining, observation of movement of the nucleus, short time exposure	Continuous observation stresses the cell, test dissolution for species with thick test
<i>8-Hydroxypyrene-1,3,6-trisulfonic acid</i>	HPTS	pH indicator	<i>Ammonia tepida</i>	200	Living	Culture	410/470-555	Yes	Accurately measure of pH with two wavelength excitation	Long incubation, scarce permeability, selective uptakes among species, calibration curve requires
<i>LysoSensor™</i> Green <i>DND-189</i>	LysoSensor™	Acidic vesicles	<i>Ammonia tepida</i>	20	Living	Natural samples	443/595	Yes	Suitable for live staining, easy staining procedure, membrane permeable	Relatively rapid fading
<i>MitoTracker®</i> Green FM	N/A	Mitochondria	<i>Amphistegina lessonii</i> , <i>Amphistegina</i> sp., <i>Bolivina variabilis</i> and <i>Quinqueloculina</i> sp.	100	Living	Culture	490/516	Yes	Suitable for live staining, easy staining procedure, membrane permeable, absorption/emission spectra differ from chlorophyll (suitable for symbiotic species)	Signal may overlap with autofluorescence (especially in miliolids)
<i>MitoTracker®</i> Red <i>CMXRos</i>	N/A	Mitochondria	<i>Ammonia tepida</i>	20	Living	Natural samples	579/599	No	N/A	Scarce or no permeability
<i>MitoTracker®</i> Red FM	N/A	Mitochondria	<i>Amphistegina</i> sp., <i>Bolivina variabilis</i> and <i>Quinqueloculina</i> sp.	100	Living	Culture	579/599	Yes	Suitable for live staining, easy staining procedure, membrane permeable	Relatively rapid fading
<i>Nile Red</i>	NR	Neutral and Polar lipids	<i>Ammonia parkinsoniana</i>	100	Fixed and Living	Natural samples and culture	Red 488/ > 590 Yellow 488/570-590	Yes	Suitable for live staining, easy staining procedure, membrane permeable	Broad emission spectra
<i>Nonyl Acridine Orange</i>	NAO	Mitochondria	<i>Ammonia tepida</i>	20	Living	Natural samples		No	N/A	Scarce or no permeability

**Table 1**  
(continued)

Probe name	Acronym	Application	Foraminiferal species	Number of specimens	Status	Foraminiferal specimens	Excitation/Emmission (nm)	Applicability	Pros	Cons
<i>NucRed™ Live 647 ReadyProbes™ Reagent</i>	NucRed™	Nucleic Acids, Nucleus	<i>Ammonia tepida</i>	20	Living	Natural samples	491-497/ 515-523	No	N/A	Sease or no permeability
<i>Rhod-3 acetoxymethyl ester</i>	Rhod-3AM	Calcium	<i>Ammonia tepida</i>	100	Living	Culture	550/600	Yes	Simultaneous observation of Ca and pH with double staining	Possible overlap with the autofluorescence of chlorophyll, appropriate band pass filter required
<i>SiR-actin</i>	N/A	F-Actin	<i>Amphistegina lessonii</i>	100	Living	Culture	652/674	Yes	Suitable for live staining, easy staining procedure, membrane permeable	Absorption and emission spectra overlapping with spectra of chlorophyll, possibility of induction of F-actin polymerization
<i>SiR-tubulin</i>	N/A	Microtubule	<i>Amphistegina lessonii</i>	20	Living	Culture	652/674	Yes	Suitable for live staining, easy staining procedure, membrane permeable	Absorption/emission spectra overlapping with spectra of chlorophyll
<i>DYLight 554-phalloidin</i>	N/A	F-Actin	<i>Amphistegina lessonii</i>	10	Fixed	Culture	652/675	Yes	Gold standard for visualizing F-actin	High toxicity, membrane impermeable, hardly suitable for live staining

Note. N/A = not applicable; NR = Nile Red; NAO = Nonyl Acridine Orange.

All specimens were gently brushed with a fine brush to remove algae and fine grains of sediment from the surface of the test before probes' testing. The number of tested specimens for each probe is reported in Table 1. The viability check of foraminiferal specimens was based on their pseudopodial activity.

### 3.2. Autofluorescence Evaluations

Background fluorescence and autofluorescence are important issues for cell imaging. The former is commonly due to fluorescent compounds that are not completely rinsed away from the medium, while the latter is caused by the natural emission by biological structures such as symbionts and organelles such as chloroplasts and mitochondria. Autofluorescence might severely compromise the application of fluorescence microscopy by interfering with probe signal detection (Neumann & Gabel, 2002). Detection of autofluorescence can be minimized by performing a correct preliminary evaluation and selecting appropriate filters and alternative probes with excitation/emission wavelengths that differ from the autofluorescent agent(s). Reduction of background fluorescence can be achieved by extended rinses and multiple washings.

Living benthic foraminifera can emit autofluorescence; therefore, the application of fluorescent and fluorogenic probes and their detection cannot be reliably evaluated without the documentation of autofluorescence. In this evaluation, we tested the foraminiferal autofluorescence at various wavelengths, filter-set properties (excitation: EX, emission: EM wavelengths, and band-pass filters that selectively permit the passage of the wavelengths absorbed by the probe, therefore reducing excitation of other sources of fluorescence and blocking excitation light in the fluorescence emission band) and time exposure (50, 100, 500, and 1,000 ms) using three different epifluorescence microscopes (Zeiss Axio Observer with Black/White AxioCam MRm monochrome digital camera, Keyence BZ-9000, and Olympus IX81 with Hamamatsu B/W ORCA-R2 C10600-10B digital camera).

*Ammonia beccarii* was chosen for this evaluation because this taxon is one of the most common. Living specimens of this species were placed in Petri dishes containing 0.2- $\mu$ m filtered (mixed cellulose ester membrane filter, Advantec) seawater collected from the open ocean in Sagami Bay, Pacific Ocean (salinity ~35). Dishes were kept at room temperature (RT; ~20 °C) under daily light/dark conditions (12-hr light/12-hr dark). Twice a week, specimens were fed with living microalgae (*Dunaliella* sp.); seawater was replaced weekly to avoid accumulation of waste products. To evaluate autofluorescence, specimens were not fed for a week to minimize autofluorescence from chlorophyll of ingested algae. Then, living specimens of fed and unfed *A. beccarii* were marked with different sets of probes for each microscope and camera combination. *SNARF-1*, *DsRed*, *GFP*, *DAPI*, *Fura-2*, *Fura-2*, and *HTPS* were assessed with the Axio Observer (Zeiss); *GFP-B*, *TRITC*, *DAPI-B*, and *Cy5* were assessed with a Keyence BZ-9000 microscope. *WIB* and *WIG* were assessed with an Olympus ZWQ microscope. All combinations were assessed at different exposures (50, 100, 500 ms, and 1 s; Table 2).

### 3.3. Confocal Laser Scanning Microscopy Analyses

For confocal laser scanning microscopy (CLSM), living specimens of *A. tepida* were treated with a set of probes depending on process to be assessed, following specific incubation protocols as discussed in further detail below. All probes were obtained from Thermo Fisher Scientific (Massachusetts, United States; For probe details, please refer to Johnson & Spence, 2010). A Leica Microsystems TCS SP5 II CLSM with 488-, 543-, and 663-nm excitation illumination and oil-immersion objectives was used. The images were further processed, as required, in ImageJ software (National Institutes of Health, Bethesda, MD, United States).

#### 3.3.1. Oxidative Stress

As a response to oxidative stress, cells in aerobic organisms increase the production and release of reactive oxygen species (ROS) in their cytoplasm (McBee et al., 2017; Takahashi et al., 2001). CellROX® Green is a membrane-permeable probe used to detect ROS within a cell. This fluorogenic probe is almost nonfluorescent when in a reduced state and shows a bright fluorescent signal when it is oxidized. Thus, unstressed cells with a low production of ROS show a low fluorescence signal, while when the production of ROS increases due to an oxidative stress condition, cells show a higher fluorescence (McBee et al., 2017). This probe can be used in both living and fixed cells. In this study, CellROX® Green was only used in living cells.

CellROX binds to free radicals in the cytoplasm; hence it was used to compare the quantity of ROS in both unstressed and stressed cells. Specimens used as negative control (i.e., pH 7.8, unstressed) were washed with artificial sea water (ASW) and directly incubated in 5  $\mu$ M CellROX® Green for 60 min at RT, whereas another

**Table 2**

List of Probes for Autofluorescence Evaluation Including Microscopy, Excitation, FT (“Farb Teiler”, i.e., Color Splitter), Emission, and Exposure

Probes	Microscopy	Excitation	FT	Emission	Exposure
		(nm)		(nm)	(ms)
SNARF-1	Axio Observer	510/25	540	580/30	50, 100, 500, and 1,000
SNARF-1		510/25	610	640/35	
DsRed		550/25	570	605/70	
GFP		470/40	495	525/50	
DAPI		365	395	445/50	
Fura-2		340/80	409	510/90	
Fura-2		387/15	409	510/90	
HTPS		410/30	500	535/48	
HPTS		470/20	nd	535/48	
GFP-B	Keyence XYZ	470/40	495	535/50	
TRICT		540/25	565	605/55	
DAPI-B		360/40	400	460/50	
Cy5		620/60	660	700/75	
WIB	Olympus ZWQ	477/35	505	510	
WIG		540/10	570	575	

group of specimens was first incubated at increased pH (9.5) for 60 min, after which these specimens were rinsed with ASW and incubated in CellROX® Green following the same procedure as the unstressed group. Then, both unstressed and stressed individuals were subject to blue excitation (500 nm) and analyzed for green fluorescent emission (525 nm) using CLSM.

### 3.3.2. Neutral and Polar Lipids

Neutral lipids (i.e., esterified cholesterol and triglycerides) are stored in lipid droplets (LDs; Guo et al., 2009), structures used as compartments to store excess lipids by the cell on the basis of its natural metabolism (Frontalini et al., 2018). These LD can be defined as lipid ester cores with a surface delimited by a phospholipid monolayer. High-content screening (HCS) LipidTOX™ is a probe developed to have a high affinity for neutral lipids, enabling their accurate detection and quantification in fixed cells.

Selected specimens of *A. tepida* were prepared for CLSM by rinsing with ASW and fixing with 2% paraformaldehyde for 2 hr. Subsequently, samples were washed in ASW and decalcified with Ethylene Diamine Tetra Acetic Acid (EDTA) (0.1 M) for 48 hr to remove the calcareous foraminiferal test. Upon decalcification, specimens were incubated in LipidTOX™ (10 times) for 1 hr and mounted for scanning with CLSM. Specimens were excited with blue light at 495 nm, and their green fluorescence was imaged at 525-nm emission.

NR is a phenoxazine probe used on living and fixed cells to localize and quantify neutral and polar lipids (Greenspan & Fowler, 1985; Sackett & Wolff, 1987). The fluorescence properties of NR are known to be sensitive to environmental factors such as polarity of lipids. Polar lipids (i.e., phospholipids), which are mostly present in membranes, fluoresce red (emission >590 nm), whereas neutral lipids fluoresce yellow (570–590 nm) after excitation at 488 nm (Diaz et al., 2008; Greenspan et al., 1985). Previously, NR was used on *A. parkinsoniana* to detect membranous vesicles and to compare the lipidic distributions of specimens with or without exposure to Hg (Frontalini et al., 2016).

Briefly, for NR microscopy, *A. parkinsoniana* specimens were fixed in 2% paraformaldehyde for 2 hr, then washed in ASW and decalcified with EDTA (0.1 M) for 48 hr to remove the foraminiferal test. Following decalcification at RT, specimens were rinsed in ASW, and NR was added at a final concentration of 3 µg/ml, for 40 min. Using CLSM, specimens were subject to blue excitation (488 nm) and analyzed separately for the two different emissions (for the whole protocol and experiment see Frontalini et al., 2016).

### 3.3.3. Golgi Complex

The Golgi complex (also called apparatus, body, or the “Golgi”) is responsible for transporting, modifying, and packaging proteins and lipids into membrane-bound vesicles inside the cell. It receives proteins and lipids from the rough endoplasmic reticulum at the *cis* face and dispatches vesicles to lysosomes, to the cell membrane or outside its *trans* face. The Golgi is made up of multiple membranes called cisternae, which are held together by matrix proteins and supported by cytoplasmic microtubules. The red

fluorescent *BODIPY<sup>TM</sup> TR C5 ceramide complexed to BSA* (hereafter referred as *BODIPY<sup>TM</sup>*) is a probe used to identify sphingolipid transport and metabolism mechanisms while the ceramide analogs selectively the Golgi complex. *BODIPY<sup>TM</sup>* is a red fluorescent cell label (excitation/emission maxima ~589/617 nm). This probe can be used in living or fixed cells, which were both tested in the present study. Selected specimens were prepared for CLSM by rinsing with ASW and then fixed with 2% paraformaldehyde for 2 hr and rinsed again in ASW. Specimens were then decalcified with EDTA (0.1 M) for 48 hr to remove the test. Decalcified specimens were incubated in *BODIPY<sup>TM</sup>* for 60 min at a concentration of 5  $\mu$ M at RT and then scanned with CLSM.

#### 3.3.4. Lysosomes

Lysosomes are membranous vesicles containing hydrolytic enzymes; lysosomes have fundamental roles in cell digestion and autophagy, as they fuse with food vacuoles, redundant or damaged organelles, and proteins (Anderson & Lee, 1991; Yorimitsu & Klionsky, 2005). To study dynamic changes and function(s) of the lysosomes, the fluorescent *LysoSensor<sup>TM</sup> Green DND-189* was used. *LysoSensor<sup>TM</sup>* probes are pH-dependent where the acidotropic dye accumulates inside acidic vesicles due to protonation, meaning that the fluorescence intensity increases proportionally to acidification (Lu et al., 2017).

In this case, the probe must be used on living cells. Therefore, selected individuals of *A. tepida* were rinsed with ASW and then incubated with 1-mM *LysoSensor<sup>TM</sup> Green* for 60 min at RT. Upon incubation, samples were analyzed with CLSM. After excitation at 443 nm, emitted green fluorescence was imaged at 505 nm.

The pH-sensitive dye AO was also used to detect and quantify acidic vesicular organelles in *A. parkinsoniana* by CLSM (Frontalini et al., 2016). AO is a cell-permeable fluorescent dye that labels DNA and cytoplasm bright green, whereas RNA and acidic vacuoles appear red. AO can enter acidic compartments and organelles, such as lysosomes and autolysosomes, where it becomes protonated and sequestered (Traganos & Darzynkiewicz, 1994). When AO is bound to acidic compartments emits red fluorescence (>650 nm) with an intensity proportional to the acidity.

Live *A. parkinsoniana* specimens were incubated in AO (150 ng/ml) for 40 min at RT. After blue (488) excitation, green and red fluorescence emissions were imaged with CLSM. Because AO must be used on living specimens and foraminiferal tests may interfere with its uptake, only signals at the cell periphery were observed (Frontalini et al., 2016).

#### 3.3.5. Cytoskeleton Structures

The foraminiferal cytoskeleton is composed of microtubules and microfilaments of actin (Travis & Bowser, 1991). There are several methods to mark cytoskeletal structural components of cytoskeleton in either fixed or living specimens.

##### 3.3.5.1. Actin Microfilaments

*ActinGreen<sup>TM</sup> 488 ReadyProbes<sup>®</sup>* is a conjugation of a high affinity F-actin probe and bright green photo-stable Alexa Fluor<sup>®</sup> 488 resulting in a fluorescent membrane-permeable probe that strongly binds to F-actin (Goulding et al., 2014). It has a higher affinity for this protein than antibody-based methods. *ActinGreen<sup>TM</sup> 488 ReadyProbes<sup>®</sup>* has to be used on previously fixed and permeabilized cells. *Ammonia tepida* specimens were rinsed before and after fixation with 2% paraformaldehyde. On the first attempt, the specimens were permeabilized with 0.1% saponin and then incubated with *ActinGreen<sup>TM</sup> 488 ReadyProbes<sup>®</sup>* for 1 hr, according to the manufacturer's instructions, and then imaged with CLSM (495-nm emission; 518-nm emission). This procedure was unsuccessful, so a second attempt used Triton X-100 to permeabilize the cell membrane. This attempt was successful.

*SiR-actin* is a new fluorogenic probe designed for live-cell imaging of actin. This probe is based on the fluorophore silicon rhodamine (*SiR*) and the actin binding natural product jasplakinolide (Lukinavičius et al., 2014). *SiR-actin* is cell permeable to live cells, allowing labeling of F-actin with high specificity and a low level of background fluorescence (Lukinavičius et al., 2014) that permitted imaging without removal of excess probe through rinsing. Its far-red excitation (652 nm) and emission (674 nm) wavelengths are non-toxic for living cells. A 1-mM stock solution was prepared by dissolving *SiR-actin* in anhydrous dimethyl sulfoxide. F-actin was labeled with *SiR-actin* following the procedure described by Lukinavičius et al. (2014) and tested on foraminifera by Tyszka et al. (2019). *Amphistegina lessonii* specimens were incubated with 2- $\mu$ M *SiR-actin* in growth medium at 21–23 °C for 30 min. The growth medium contained natural sea water (NSW) with a salinity of 32 and pH of 8.2. Small *A. lessonii* individuals were selected to



facilitate observation and labeling of several individuals in the same imaging Petri dish with either a glass or polymer coverslip bottom (supplied by ibidi®).

Live specimens were labeled to monitor a complete process of chamber formation. All experiments followed the same procedures and were replicated using different individuals at different chamber-formation stages. Temporal sequences were observed and recorded using a Zeiss Axio Observer.Z1 equipped with Apotome.2, a software module for optical sectioning that applies structured illumination microscopy, and a Leica SP5 camera.

*Phalloidin* is the most popular probe to locate actin in fixed cells. *Tetramethylrhodamine (TMR-)phalloidin* (Molecular Probes, United States) was used for marking pseudopodial networks in *Allogromia* sp. Two permeabilization and fixation procedures were used. In the first procedure, specimens of *Allogromia* were fixed with glutaraldehyde and then permeabilized with Triton X-100 (see Bowser et al., 1988 for details). In the second option, specimens were lysed with nonionic detergents, prior to fixation, into buffers reported to stabilize actin microfilaments in nonmuscle cells (Bowser et al., 1988; Schliwa & van Blerkom, 1981; Travis & Allen, 1981). Specimens were then incubated in  $3 \times 10^{-7}$  M *TMR-phalloidin* (Bowser et al., 1988; Travis & Bowser, 1986a, 1986b), after which tests were decalcified with EDTA (0.1 M) for 48 hr.

Actin labeling in foraminifera can partly also follow procedures applied to diatoms by van de Meene and Pickett-Heaps (2002), as well as Tesson and Hildebrand (2010). In our study, foraminifera were fixed at 4 °C in 4% methanol-free formaldehyde prepared in Actin Stabilizing Buffer (ASB—10 mM PIPES/10 mM EGTA/5 mM MgSO<sub>4</sub>/pH 8.0) containing 100 μM MBS (m-maleimidobenzoyl N-hydroxysuccinimide ester) and 3% NaCl. Specimens were then rinsed twice in ASB buffer and labeled with *DYLight 554-phalloidin* (Cellomics Cytoskeletal Rearrangement Kit, Thermo Fisher Scientific) diluted at 1/100 in ASB buffer for 2 hr at RT. Samples were then rinsed twice in ASB and kept in ASB for observations using a Leica Confocal SP2 equipped with a UV laser (Coherent) and a neon/red laser. The round cover glasses with attached and labeled foraminifera were transferred to HYDRO-BIOS plate chambers for all observations. Samples can be kept for a few weeks when stored at 4 °C in the dark.

#### 3.3.5.2. Tubulin Microstructures

In fixed specimens, microtubules and other tubulin-containing structures (see section on actin phalloidin labeling) can be marked using a commercial tubulin antibody (Rupp et al., 1986) and visualized using fluorescein isothiocyanate-conjugated secondary antibodies (Sigma). Double labeling of actin and tubulin was applied to study co-localization of cytoskeleton structures in the foraminifer *Allogromia laticollaris* (Bowser et al., 1988). Actin/tubulin double labeling may also follow procedures applied to diatoms by van de Meene and Pickett-Heaps (2002), as well as Tesson and Hildebrand (2010). Actin-labeled fixed specimens (see above) were rinsed twice in ASB and incubated in the secondary antibody staining solution (5 μl DyLight 649 Goat Anti-Mouse +5 ml of ASB) while protected from light for 30–60 min. Samples must be washed three times with ASB and kept in ASB for fluorescence observations.

*SiR-tubulin* live staining has also been tested recently. SiR-tubulin is based on the fluorophore silicon rhodamine (*SiR*) conjugated to the microtubule binding drug Docetaxel (Lukinavičius et al., 2014). This probe labels microtubules in live cells with high specificity and low background. Its far-red excitation (652 nm) and emission (674 nm) wavelengths, like in SiR-actin, are nontoxic to living cells (Lukinavičius et al., 2014). The growth medium and labeling protocol followed that described for SiR-actin staining (see above and follow *Spirochrome* product information: SiR-tubulin Kit, CY-SC002).

#### 3.3.6. Mitochondria

Mitochondria are double-membrane organelles that function as centres of ATP production (Anderson & Lee, 1991). MitoTracker cell-permeant probes are mitochondrial-selective fluorescent labels commonly applied in fluorescent CLSM and flow cytometry (Presley et al., 2003). These probes selectively accumulate in the mitochondrial matrix by covalent binding to mitochondrial proteins (Presley et al., 2003).

MitoTracker® Red CMXRos, a cationic fluorophore that accumulates into mitochondria, was used to localize and mark these organelles within the cell. This membrane-permeable probe reaches the matrix inside mitochondria due to the negative membrane potential of mitochondria (Kholmukhamedov et al., 2013), and it is retained inside the organelle because of the covalent bond created between its chloromethyl group and thiols on proteins and peptides. This probe must be used on living cells. In order to test the validity of MitoTracker® Red CMXRos, specimens of *A. tepida* were rinsed with ASW prior to treatment and incubated with the probe

at a final concentration of 300 nM for 60 min at RT. This probe passively diffuses across the plasma membrane. After a rinse in ASW, samples were excited at 579 nm and observed at 599-nm emission.

MitoTracker® Green FM and MitoTracker® Red FM are recommended for live cell labeling (Invitrogen manual downloaded on 25 June 2018 from <https://assets.thermofisher.com/TFS-Assets/LSG/manuals/mp07510.pdf>). These probes passively diffuse across the plasma membrane and accumulate in active mitochondria. A 1-mM stock solution was prepared with dimethyl sulfoxide. Mitochondria were labeled by incubation with either probe (MitoTracker® Green FM; MitoTracker® Red FM). Both probes were tested on living foraminifera incubated in seawater at a concentration of 1  $\mu$ M for at least 30 min at RT. After incubation, specimens were rinsed with seawater. *Quinqueloculina* sp. and small *A. lessonii* were used for experiments. Specimens were labeled with MitoTracker® Green FM and MitoTracker® Red FM then analyzed using Zeiss Axio Observer.Z1 and Leica SP5 CLSM, respectively. For excitation of MitoTracker® Green FM, we used blue light within the range of 460–490 nm; emissions were observed over a range of 500–600 nm. Specimens incubated with MitoTracker® Red FM were excited at 581 nm and observed over the range of 650–691 nm. MitoTracker® Red FM emission overlaps with the autofluorescence of chlorophyll, which can be in symbionts and algal food remnants.

Nonyl Acridine Orange (Acridine Orange 10-Nonyl Bromide, NAO) is a fluorescent probe derived from Acridine Orange, which is retained inside mitochondria (Petit et al., 1992); this compound passes through the outer mitochondrial membrane and binds to negatively charged phospholipids (cardiolipin, phosphatidylinositol and phosphatidylserine; Petit et al., 1992). NAO can be used on both living and fixed cells. Specimens of *A. tepida* were rinsed with ASW, incubated with NAO for 60 min at RT, and subsequently washed again with ASW. After the incubation and rinse, the specimens were examined with CLSM using 495-nm excitation (blue) and 520-nm emission (green).

### 3.3.7. Nuclei

The NucRed™ Live 647 ReadyProbes™ Reagent, which emits in the far-red range, is widely used for labeling nuclei in live or fixed cells. Specimens of *A. tepida* were rinsed with ASW, incubated with 2 drops/ml NucRed™ Live 647 ReadyProbes™ Reagent for 60 min at RT, and subsequently washed again with ASW. After incubation, the specimens were examined with CLSM at 638-nm excitation and 686-nm emission.

## 3.4. Optical Sectioning Structured Illumination Microscopy Analyses

Additionally, we conducted tests on other species of foraminifera, namely *Amphistegina* sp., *Bolivina variabilis* and *Quinqueloculina* sp. In order to avoid interference with autofluorescence from symbiotic or digested algae, we only focused on mitochondrial movement along the pseudopodia. Juvenile specimens of *Amphistegina* sp. and *Quinqueloculina* sp. were transferred from a culture aquarium to a Petri dish. Using a binocular microscope, individuals that moved were transferred to an ibidi® Polymer Coverslip Bottom and incubated for 1 hr in MitoTracker® Green FM with a final concentration of 2  $\mu$ M in natural sea water (NSW). After incubation, the specimens were observed with a Zeiss AxioObserver Z.1 microscope equipped with the Apotome.2 module using structured illumination principles to create optical sections of specimens, thereby removing scattered light (Chasles et al., 2007).

To assess autofluorescence of *Quinqueloculina* sp., we performed a parallel labeling experiment in separate Petri dishes with two different dyes: MitoTracker® Green FM labeling mitochondria and CellTrace™ Calcein Red-Orange, AM marking cytoplasm. Before incubation, specimens were gently brushed with a fine brush to remove algae and grains of sediment from the surface of the test, then they were rinsed with ASW. Active (motile) individuals were separately transferred into two Petri dishes containing different staining solution: in the first dish: MitoTracker® Green FM with a final concentration of 2  $\mu$ M in NSW prepared following manufacturer's instructions, and in the second CellTrace™ Calcein Red-Orange, AM with a final concentration of 2  $\mu$ M in NSW also prepared following manufacturer's instructions. After incubation all individuals were washed with clean NSW and transferred to an imaging dish with a ibidi® Polymer Coverslip Bottom. For imaging, the Zeiss AxioObserver Z.1 microscope equipped with the Apotome.2 module was used.

## 3.5. Conventional Wide-Field Fluorescence Microscopy

### 3.5.1. Nuclei

Hoechst 33342 (H3570, Thermo Fisher Invitrogen, United States) allows visualization of foraminiferal nuclei (Bernhard & Bowser, 1992). This is a useful probe for tracking the movement of the nuclei within the

foraminifera. Though the dye itself is cell permeable, the calcareous test may be dissolved before incubation for a clearer observation. Living *Ammonia* individuals were placed in Ca-free ASW for three days to dissolve their test (Toyofuku et al., 2008). During decalcification, changes in chamber arrangement can occur, but this does not interfere with nuclear observation. In darkness, specimens were then incubated with 5  $\mu\text{g}/\text{ml}$  Hoechst 33342 seawater solution for 30 min and then rinsed in ASW. This probe can be visualized with conventional DAPI settings of an inverted microscope equipped with Epi-illumination (i.e., 335- to 383-nm excitation; 420- to 470-nm emission). Hoechst 33342 was also tested in *Spirillina vivipara* where test dissolution was not necessary to visualize nuclei. Because the test of *S. vivipara* is thinner ( $\sim 1 \mu\text{m}$ ) than the test of *Ammonia* ( $> 10 \mu\text{m}$ ), Hoechst 33342 may penetrate more readily in the former.

### 3.5.2. Calcification

To investigate the calcification process in foraminifera, it is necessary to visualize the distribution of both calcium and carbonate ions. Various reagents are commercially available for visualization of the former, while there is no method available to our knowledge that visualizes the latter. Carbon ion speciation in seawater is governed by pH and many methods are available to detect pH variations using fluorescence. Once pH is visualized, it is possible to quantitatively estimate the speciation of the carbonate system, if one other carbonate system parameter is known or can be estimated. It is important to compare the distributions of both calcium ion and carbonate ion systems to study the foraminiferal calcification process. Therefore, it is necessary to identify a combination of probes with mutually exclusive wavelengths. Here, we introduce a double labeling method with *Rhod-3 acetoxymethyl ester (Rhod-3AM)* as the calcium ion probe and pyranine as pH indicator probe. This combination of Rhod-3AM and pyranine was chosen because there is no interference of their fluorescence wavelengths.

Living *A. beccarii* were incubated at RT overnight in a cocktail of Rhod-3AM (8  $\mu\text{M}$ ; Thermo Fisher Scientific) and pyranine (20  $\mu\text{M}$ ; 8-hydroxypyrene-1,3,6-trisulfonic acid, HPTS; Sigma-Aldrich, H1529). Rhod-3AM has red fluorescence when excited by green light (Ex 550 nm; Em 600 nm), while HPTS has green fluorescence when excited by violet or blue light (Ex 410 nm; Em 470/535 nm). The incubation dish was covered with aluminum foil to reduce the risk of photo damage. Fluorescence was assessed with a Zeiss Axiovision inverted microscope equipped with Epi-illumination. In a darkened room, the Rhod-3 illumination was easily visible. Time lapse images were captured by a digital camera attached to the microscope using a standard software package. For pH quantification, grey scale images representing different excitation wavelengths were recorded. Subsequently, ratiometric pH images were calculated by dividing  $\lambda_{470}^{\text{exc}}$  by  $\lambda_{410}^{\text{exc}}$  for each pixel using a calibration curve (de Nooijer et al., 2008).

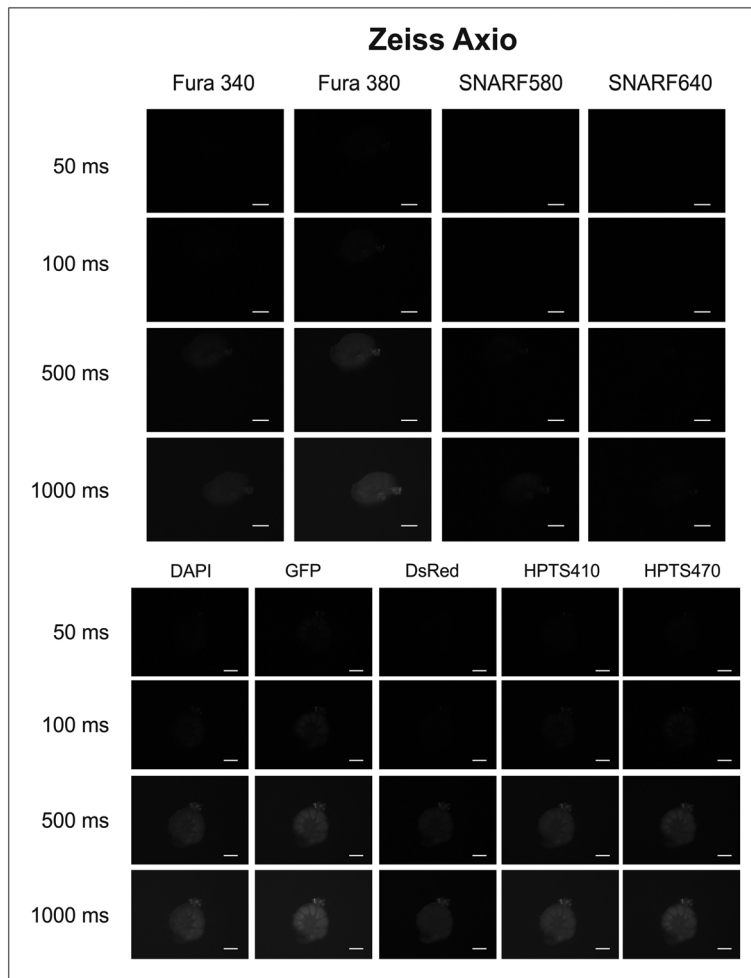
## 4. Results and Discussion

### 4.1. Autofluorescence in Foraminifera

The number of fluorescent probes applied to physiological and ecological studies of foraminifera is increasing. However, few cases have fully accounted for autofluorescence and its potential influence on the signal under investigation (Bernhard et al., 1995; Knight et al., 1985; Schwab & Schlobach, 1979). It is known that various pigments and organelles (i.e., mitochondria, lipofuscin, and lysosomes) present in the foraminiferal cell might produce autofluorescence. Furthermore, foraminifera are unicellular organisms, and the intracellular phagocytes include food-derived organic matter. For example, when microalgae are fed as food, there is a possibility that chlorophyll and its derivatives have autofluorescence. In light of this, understanding the autofluorescence of foraminifera is a prerequisite for a reliable application of fluorescent probes.

In order to evaluate foraminiferal autofluorescence, both fed and nonfed individuals of *A. beccarii* were observed (Figures 1–3 and S1–S3). The chlorophyll contained in food vacuoles and symbiotic algae likely has the strongest autofluorescence within foraminiferal cells. For this reason, we evaluated the autofluorescence of chlorophyll by observing fed *Ammonia* (Figures S1–S3). Species-specific effects should be considered when observing weaker fluorescence signals. Autofluorescence was negligible in any filter set when exposure times did not exceed 500 ms, although there was a difference in autofluorescence intensity depending on the filter sets (i.e., the wavelengths). Typically, autofluorescence, if detected, will not be problematic if the probe signal strength is sufficient.

Characteristic distributions of autofluorescence were observed with Keyence's *GFP-B* and *Cy5* filter sets in unfed individuals (Figure S2). There were many fluorescent features that might be misidentified as

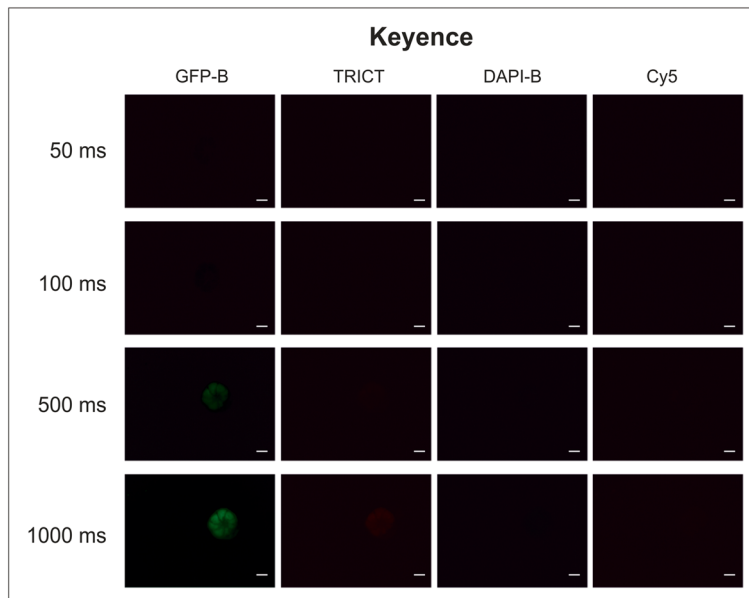


**Figure 1.** Epifluorescence images of live foraminifera to assess autofluorescence using nine band-pass fluorescence filter sets of a Zeiss AxioObserver Z1 with a B/W AxioCam MRm digital camera. Four exposure times were considered for each filter set. Foraminifera had been fed recently. Autofluorescence (brightness) was not detected when the exposure times were 50 and 100 ms. Autofluorescence was not noted with *SNARF580* and *SNARF640* filter sets. Filters are named as acronyms of probes corresponding to the applicable wavelength. Scale bars = 100  $\mu\text{m}$ .

intracellular organelle(s). The Zeiss and Keyence microscopes that we used for this study have band-pass filters narrowing detection of signals to specific bands of wavelengths. The Olympus microscope has a long-pass filter, which allows all wavelengths exceeding that of the emission filter. Observations with band-pass filters show less nonspecific fluorescence (Figures 1, 2).

On the other hand, observations with long-pass filters show relatively stronger autofluorescence that could be related to the presence of fed microalgae (Figure 3). Additional observations on unfed individuals revealed that the autofluorescence intensity weakens over time and the intracellular distribution also changes from diffuse to granular over 1 week (Figure S2).

On the basis of our results, autofluorescence was present in the foraminiferal cell itself (Figures 1–3), but only when exposure time exceeded one half second. Specifically, when the exposure time is long, autofluorescence might occur. In addition to it, it is necessary to consider the possible interference with autofluorescence of chlorophyll *a* of algal food materials and/or symbiotic algae (Figure 3). On the other hand, because the autofluorescence of foraminifera is not markedly evident in our results (Figures 1 and 2), if the signal of the fluorescent probe is sufficiently strong and the exposure time is short, the probe may be correctly applied. It is, however, recommended to investigate the autofluorescence of the targeted foraminifera with the filter set of each probe for the specific observation.

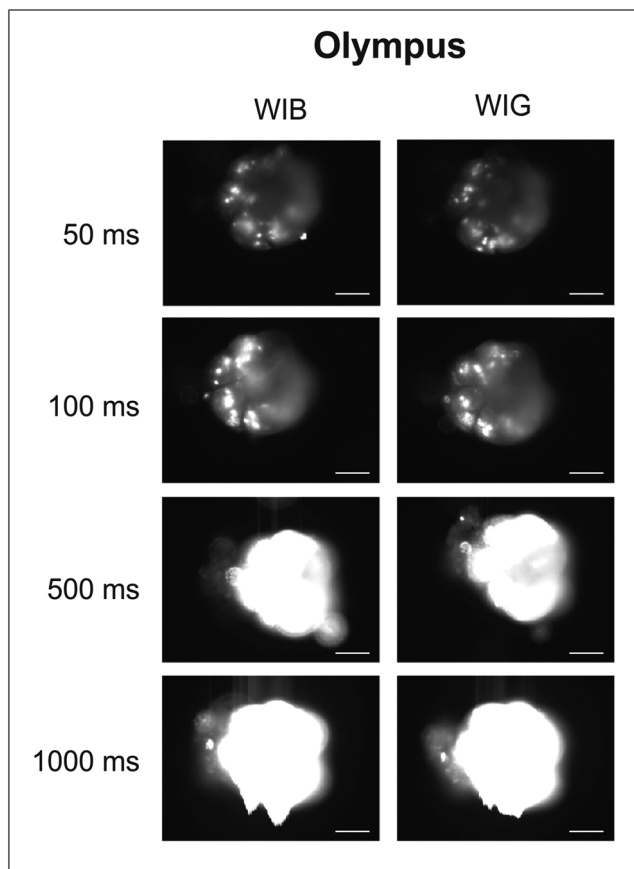


**Figure 2.** Epifluorescence images of live foraminifera to assess autofluorescence using four fluorescent filters from Keyence BZ-9000 equipped with color camera. Four exposure times were considered for each filter set. Foraminifera had been fed recently. Autofluorescence (brightness) was negligible except for 500 and 1,000 ms of exposure times with *GFP-B*. Filters are named as acronyms of probes corresponding to the applicable wavelength. Scale bars = 100  $\mu\text{m}$ .

#### 4.2. CellHunt™ Blue as a Viability Indicator

Specimens of *A. tepida* treated with CellHunt™ Blue CMHC (CHB) were observed through an inverted microscope (Nikon Eclipse TS100) to check its accuracy as a viability indicator. Bright blue fluorescent individuals showed signs of pseudopodial activity, proof of the good vital status of the cell. The widespread use of the viability probe CellTracker™ Green CMFDA (CTG) emits fluorescence in the same wavelength of other probes (i.e., HCS LipidTOX™ Green, NAO, MitoTracker® Green, and ActinGreen™ 488 Ready Probes®), and the CHB might represent a valid alternative for marking living benthic foraminifera in the sediment and avoid the overlap with other probes. The CTG and CHB are products from the CellTracker/CellHunt family. They are both thiol reactive, cell permeant fluorogenic probes that easily pass through cell membranes and are converted to the highly fluorescent probes. Because we did not perform statistical analyses, its effectiveness and specificity require further exploration. There have been many attempts to develop a reliable method for distinguishing living foraminifera from dead ones. Methods can be classified as “terminal” and “nonterminal.” Included in the first group are the *Rose Bengal (RB)*, *Sudan Black B*, ATP assay, and ultrastructural observations, while “nonterminal” methods include direct observations of pseudopodial activity, negative geotaxis (reviewed in Bernhard, 2000), and fluorescent probes such as CTG (Bernhard et al., 2006; Bernhard & Bowser, 1996), FISH (Borrelli et al., 2011), or Calcein AM (Ohno et al., 2016). So far, the RB and the CTG are the most widely used dye/probe. The RB is commonly recommended due to its simplicity for foraminiferal monitoring studies (Schönfeld et al., 2012), but it stains proteins so will stain dead biological materials (Bernhard et al., 2006). The CTG is a methodology which, in contrast to the application of RB, is meant to be used in living cells or prior to fixation.

Several comparisons between RB and CTG have been carried out by Bernhard et al. (2006), Figueira et al. (2012), and Frontalini et al. (2018). Figueira et al. (2012) documented no statistically significant differences between the two methods in stained faunas composed mainly of agglutinated forms from a salt marsh, whereas Bernhard et al. (2006) found a significant difference between the two methods, as on average, less than half of RB stained calcareous foraminifera were proved to be living at the time of collection. The difference between environments and faunas must be taken into account while comparing the methods, as they are not representative for all conditions (Bernhard et al., 2006). Nonterminal methods are required for ensuring the viability of samples to be used. The presence of cytoplasm is not reliable and the activity of



**Figure 3.** Epifluorescence images of live foraminifera to assess autofluorescence using two fluorescent filters from an Olympus IX81 with a Hamamatsu B/W ORCA-R2 C10600-10B digital camera. Four exposure times were considered for each filter set. Foraminifera had been fed recently. Autofluorescence (brightness) was strong. Filters are named as acronyms of probes corresponding to the applicable wavelength. Scale bars = 100  $\mu\text{m}$ .

pseudopodia is too time consuming. FISH does not allow to reuse the same samples again and is difficult when investigating large volumes of sediment (Borrelli et al., 2011). Calcein AM is not retained in the cytoplasm 24 hr after incubation making the timing a difficulty. Hence, Cell Tracker/Hunt family dyes are useful for these kinds of studies. The CHB is not widely used, though it was helpful in some studies such as for the determination of the vital state of the fungus *Aureobasidium pullulans* (Nelson et al., 2000). Interestingly, Martínez et al. (2014) used CHB as a viability test in microplanktonic algae, but this was only successful for two species of nanoflagellates and one species of dinoflagellate.

#### 4.3. Oxidative Stress

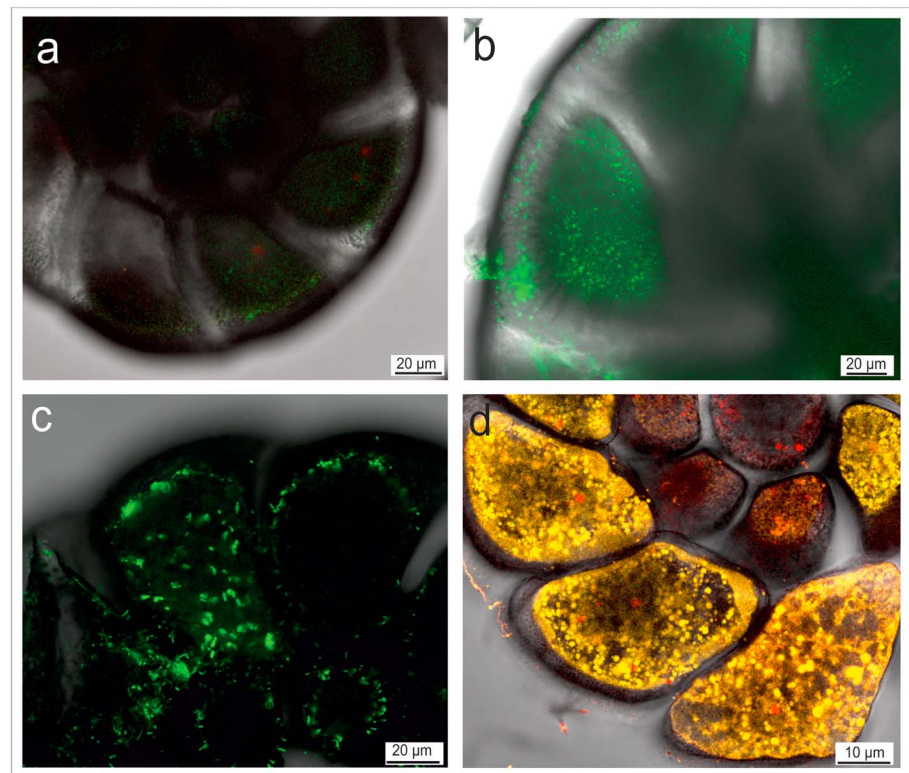
In our study, CellROX<sup>®</sup> Green was used for the first time in foraminifera to detect the presence of oxidative stress. An increase of fluorescence was found in pH stressed specimens. In fact, CLSM images of nonstressed *A. tepida* showed a dim green fluorescence (Figure 4a). Conversely, specimens subjected to higher pH (i.e., stress) exhibited a distinct bright green fluorescence that indicates increased production and occurrence of ROS or free radicals ( $\text{O}_2^-$ ,  $\text{OH}^-$ , and  $\text{H}_2\text{O}_2$ ; Figure 4b). Two different types of fluorescence were noted: (1) well-defined vesicles and (2) diffuse label. The vesicles might represent mitochondria or peroxisomes, the major ROS producers in the cell (see below), while the diffuse fluorescence is the CellROX<sup>®</sup> Green molecules bound to free radicals that are unconstrained in the cytoplasm. Red autofluorescence was detected from symbiotic microalgae present in the specimens.

Production of ROS is something that occurs naturally in cells as by-products of normal metabolic reactions, although an increase of this production is promoted by stressful conditions. The effects of harmful antibiotics were considered a cause of oxidative stress in *Escherichia coli* (Choi et al., 2015), temperature and butanol increased the production of ROS in the cyanobacteria *Synechocystis* sp. (Kaczmarzyk et al., 2014), and fibrotic pathologies such as scleroderma were linked to increased oxidative stress in human tissues (Morry et al., 2015). In foraminifera, oxidative stress leading to cellular damage and even death was noted as a

response to environmental stress (Bernhard & Bowser, 2008). de Freitas Prazeres et al. (2011) reported an increase of ROS in the symbiont-bearing species *Amphistegina lessonii* after an acute exposure to zinc, which was confirmed by Williams and Hallock (2004) reporting oxidative stress and bleaching in *Amphistegina gibbosa* experimentally stressed by light. Frontalini et al. (2018) described dysfunctional mitochondria and an increased number of degradation vacuoles and residual bodies in foraminifera exposed to three different heavy metals, attributing this result to the increase of ROS production triggered by pollutants. Free radicals are commonly encountered in the cytoplasm close to the organelles that typically produce ROS (mitochondria, peroxisomes, and chloroplasts, if present; Lesser, 2006) allowing diffuse fluorescence from CellROX<sup>®</sup> Green to mark organelles. Different fluorescence patterns represent the response of the specimens to pH change (Figures 4a and 4b), where in reference pH conditions specimens showed minor production of ROS, whereas at higher pH (9.3) the production of ROS increased, in accordance with results described by de Freitas Prazeres et al. (2011).

#### 4.4. Neutral and Polar Lipids

Selected specimens of *A. tepida* were treated with HCS LipidTOX<sup>™</sup> Green to mark the occurrence of LDs, compartments that store excess lipids in the form of esterified cholesterol and triglycerides (neutral lipids; LeKieffre et al., 2018), existing within the cytoplasm of the foraminiferal cell. It is possible to document the HCS LipidTOX<sup>™</sup> Green signal of well-defined fluorescent green vesicles that are the LD of the specimen (Figure 4c). These LDs appear in a variety of shapes, and they are randomly distributed through all the space in foraminiferal chambers, in agreement with previous studies (LeKieffre et al., 2018).



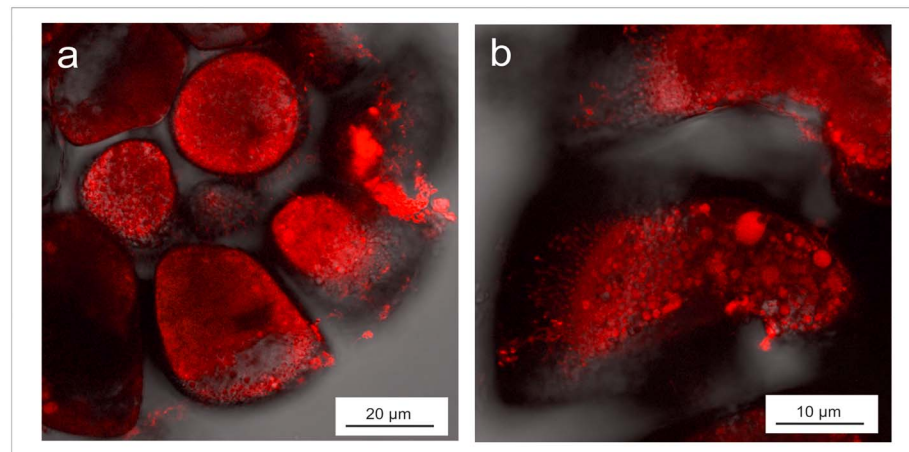
**Figure 4.** Confocal laser scanning microscopy images of foraminifera. (a) *CellROX*<sup>®</sup> *Green* of unstressed control specimens. (b) *CellROX*<sup>®</sup> *Green* of pH stressed specimen showing bright green which presumably marks ROS or free radicals. (c) *LipidTOX* signal from well-defined vesicles that are likely lipid droplets. (d) *Nile Red* label of presumed lipid droplets (yellow) and polar lipids (red).

*Ammonia parkinsoniana* specimens were treated with NR to label and distinguish neutral lipids from polar lipids (e.g., lipidic membranes) on Hg-treated and nontreated samples (Frontalini et al., 2016). The LD were labeled in yellow, whereas polar lipids are recognized as red spheres (Figure 4d). A significant increase in LDs in Hg-treated samples was described, though there was not found a significant difference in their size except for one specimen from the highest Hg concentration (Full results in Frontalini et al., 2016). These results are in accordance with findings described for other taxa exposed to adverse conditions, such as lichens facing dust pollution (Paoli et al., 2015) or grey mullet (*Mugil cephalus*) hepatocytes facing heavy metal pollution (Vasanthi et al., 2013). Le Cadre and Debenay (2006) observed an increase in number and size of LDs in benthic foraminifera as an effect of copper (Cu) contamination.

Both HCS LipidTOX<sup>™</sup> Green and NR showed their potential in characterizing lipids in benthic foraminifera. These probes have user-friendly protocols are among the most used lipid stains (Chun et al., 2013; Su et al., 2012). The HCS LipidTOX<sup>™</sup> Green and NR (among others) were compared by Chun et al. (2013) to their own developed lipid stain LipidGreen2 on zebrafish as a model. They found LipidGreen2 to produce brighter fluorescence and less nonspecific background labeling than NR and HCS LipidTOX<sup>™</sup> Green and to have higher specificity than NR. They also suggested NR as unsuitable for multicolour imaging due to its broad emission spectrum. Su et al. (2012) also compared NR and HCS LipidTOX<sup>™</sup> Green; under an alternating electrical current, they observed a more stable fluorescence of HCS LipidTOX<sup>™</sup> Green on microalgae, whereas without electrical field, NR treated samples rapidly decayed.

#### 4.5. Golgi Complex

Foraminifera incubated in BODIPY to identify Golgi showed nonspecific binding (Figures 5a and 5b). The probe apparently penetrated the foraminiferal cell, but it did not appear to selectively label the Golgi complex. The BODIPY<sup>™</sup> family of probes targets sphingolipids, a group of lipids containing the organic



**Figure 5.** (a and b) Confocal laser scanning microscopy images of EDTA-decalcified specimens of *A. tepida* after incubation with *BODIPY*<sup>™</sup>. Note the nonspecific labeling.

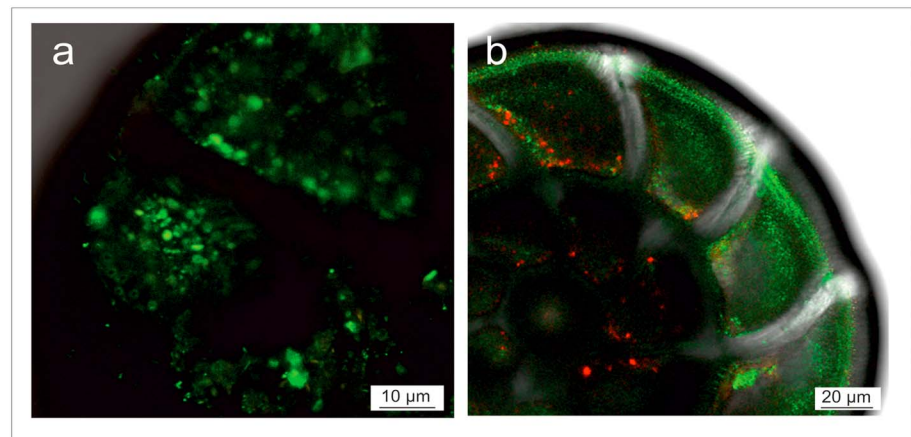
aliphatic amino alcohol sphingosine. Sphingolipids are synthesized in a pathway in the endoplasmic reticulum from nonsphingolipid precursors; synthesis is completed in the Golgi complex (Gault et al., 2010). Although sphingolipids are used for lipid trafficking in living cells, the ceramide analogs produce selective staining of the Golgi complex as structural marker. As the most effective labeling for the Golgi complex are fluorescent ceramides and sphingolipids, other probes including *CellLight*<sup>™</sup> Golgi (*GFP* or *RFP*, *BacMam 2.0*), *NBD C6-ceramide*, *NBD C6-ceramide complexed with defatted BSA*, and *BODIPY FL C5-ceramide* that can be tested on foraminifera in future experiments.

#### 4.6. Lysosomes

After treating specimens with LysoSensor<sup>™</sup> Green DND-189, CLSM images of *A. tepida* revealed numerous green acidic vesicles (presumably lysosomes, autolysosomes, and other acidic vesicles; Figure 6a). These acidic vesicles containing hydrolytic enzymes are responsible for digestion of biomolecules, damaged and redundant organelles, and proteins (Yorimitsu & Klionsky, 2005). Fluorescent vesicles are dispersed within the cytoplasm in every chamber of multilocular specimens, without a defined distribution or position in the foraminiferal chambers. Different intensities of the green fluorescence are shown in the vesicles. LysoSensor<sup>™</sup> Green DND-189 has been suggested to accumulate in acid vesicles as a result of protonation that proportionally relieves fluorescence of the molecule; hence, the most acidic vacuoles will be those with the brightest fluorescence. Hirose (1999) used LysoSensor<sup>™</sup> Green DND-189 to demonstrate that vacuoles from the tunics of *Phallusia nigra* (Asciacea) were acidic, perhaps to serve as a disinfectant. Martínez et al. (2014) tried to characterize microzooplankton assemblages with LysoSensor<sup>™</sup> Green DND-189 as a vital stain, but the probe was only successful for two species of microalgae.

To evaluate the response of *A. parkinsoniana* acidic compartments to mercury exposure, several specimens were probed with AO (Figure 6b). Specimens exposed to the highest Hg concentration displayed more conspicuous acidic compartments, likely due to vesicle volume (dimension and, as a consequence, total fluorescence intensity), when compared to those of control specimens never exposed to elevated Hg. Some of the Hg-dosed specimens also exhibited diffuse red fluorescence in their chambers, suggesting cytoplasmic acidification. After prolonged incubation, mercury-exposed specimens appeared to show an acidic compartment decrease as marked by reduction of red vacuoles suggesting a loss of lysosomal activity, a possible signal of recent or imminent death (Frontalini et al., 2016). Similar results were described in cells of other organisms, such as insects (*Aedes albopictus*; Marigómez et al., 1996), gastropod mollusk (*Arion ater*; Braeckman & Raes, 1999), or even foraminifera (Le Cadre & Debenay, 2006). Previous studies of foraminiferal lysosomes used AO to assess viability and changes in lysosome dynamics in response to xenobiotic exposure (Bresler & Yanko, 1995a, 1995b). AO is extensively used; to date, it has been used in more than 2,000 publications focused on both nucleic acids and acidic vesicles (e.g., Jensen et al., 2017; Santulli et al., 2017).





**Figure 6.** Confocal laser scanning microscopy images of foraminifera. (a) *LysoSensor*<sup>™</sup> Green DND-189, with fluorescent green acidic vesicles (lysosomes, autolysosomes, and other acidic vesicles). (b) *Acridine Orange* marks the acidic compartments in red, cytoplasm in green.

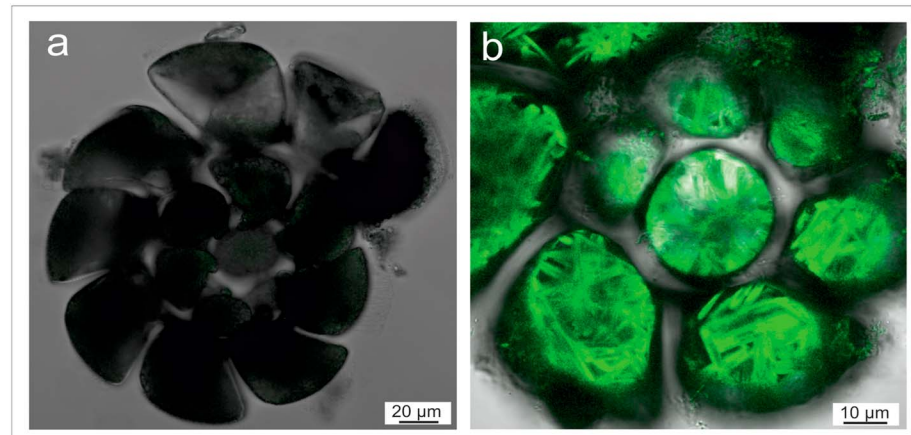
There are other fluorescence methods to track acidic vesicles in foraminiferal cells, such as *LysoTracker*<sup>™</sup>, which is a family of fluorescent compounds that accumulate inside acidic vesicles, similar to *LysoSensor*<sup>™</sup> Green DND-189 and AO; however, both their fluorescence is independent of pH (Lu et al., 2017). *LysoSensor*<sup>™</sup> Green DND-189 has never been tested on foraminifera, though promising results were reported on other taxa (e.g., Hirose, 1999; Lu et al., 2017). The use of *LysoSensor*<sup>™</sup> Green DND-189 was recommended by Wang et al. (2017) for mapping the distribution of nanoparticles in endolysosomes. It was also found to minimize artifacts due to sample manipulation produced with other classical methods such as immunofluorescence.

#### 4.7. Cytoskeleton Structures

Images obtained via CLSM showed the intratest cytoskeleton distribution in *A. tepida* labeled with *ActinGreen*<sup>™</sup> 488 Ready Probes<sup>®</sup>. We visualized bundles of foraminiferal actin microfilaments using a fluorescence method. The actin microfilaments form bundles that haphazardly traverse the cell in many directions. Some chambers appear to have more actin toward the periphery of the chamber, leaving the centre of the chamber with fewer microfilaments (Figure 7b). This result was achieved using Triton X-100 as permeabilizer before incubating the specimens with *ActinGreen*<sup>™</sup> 488 Ready Probes<sup>®</sup>. Our first attempt used a milder permeabilizer, saponin, which presumably did facilitate passage of the probe through the cell membrane (Figure 7a).

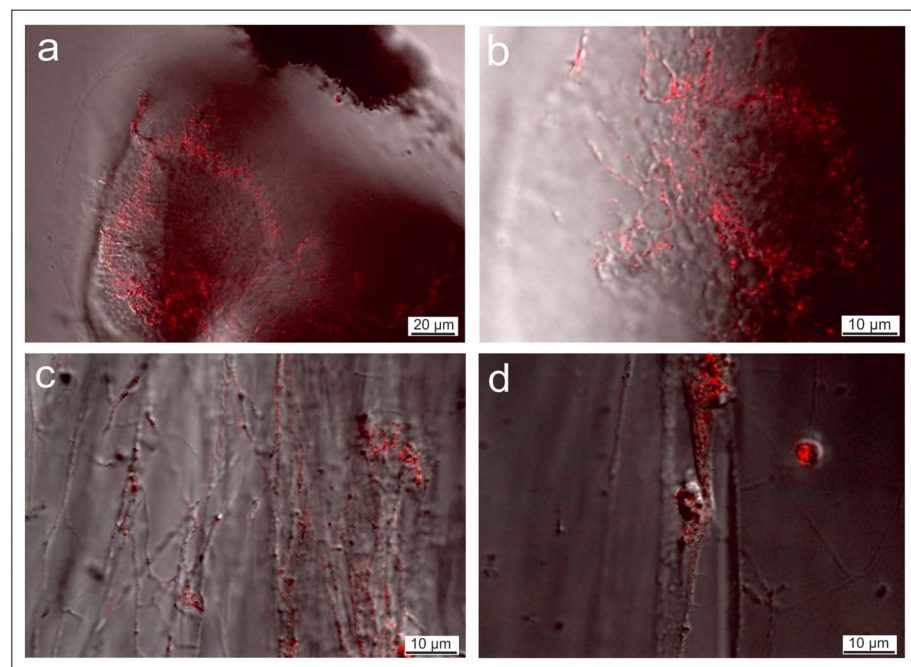
The cytoskeleton, including microtubules and actin microfilaments, is one of the most characteristic intracellular structures in foraminifera, as it is involved in essential functions, such as the formation of pseudopodia, vesicular transport, and cellular motility (Anderson & Lee, 1991; Travis & Bowser, 1991). Latest investigations indicate that F-actin meshworks associated with microtubules are highly involved in controlling morphogenesis and biomineralization (Tyszka et al., 2019). The bundles of microtubules are known to form rigid scaffolding for reticulopodia and all elongated strands (Travis & Bowser, 1986a, 1986b, 1988, 1991). Actin microfilaments tend to be concentrated toward the edges of the chambers and more condensed toward the plasma membrane due to their role in substrate adhesion, when they form actin contact plaques, so they are located on areas close to the main aperture, where the thicker pseudopodia trunks protrude (Travis & Bowser, 1991).

*ActinGreen*<sup>™</sup> 488 Ready Probes<sup>®</sup> was developed to provide an easy and reliable protocol to study F-actin distribution and dynamics within the cell. It has been used on cultured cells to understand the role of F-actin in the transport of protein degradative lysosomes and vacuoles (Zhao et al., 2014) and to discern adipogenesis differentiation mechanisms (Saben et al., 2014). Also, using animals such as mice as models (Goulding et al., 2014), *ActinGreen* has been used to characterize the distribution of F-actin in cells affected by a respiratory poxvirus.

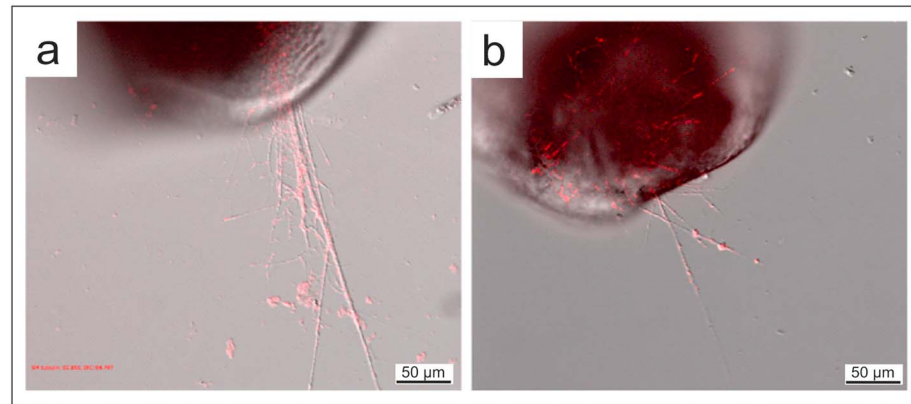


**Figure 7.** (a) *ActinGreen*<sup>TM</sup> 488 for intratest cytoskeleton distribution with saponin as permeabilizer. (b) *ActinGreen*<sup>TM</sup> 488 for intratest cytoskeleton distribution with Triton X-100 to increase permeability of the cell membrane.

SiR-actin live labeling reveals a very distinct pattern of active actin meshwork associated with most membranous surfaces of the cytoplasm. Pseudopodial structures labeled with this probe are most dynamic, presenting bidirectional movement of labeled granules (for more information see Goleń et al., 2019; Tyszcza et al., 2019). The meshwork structures show the strongest signal around the pseudopodia attachment sites to the glass or plastic substrate. Passive (immobile) structures, such as outer protective envelopes during late stages of chamber formation, do not show actin staining. The F-actin labeling (Figure 8) during chamber formation reveals a very distinct pattern with the actin meshwork present inside and outside the new biomineralized chamber. The meshwork forms a double layer enveloping the calcification fronts on both sides of the



**Figure 8.** (a) *SiR-actin* labeling of F-actin during chamber formation in *Amphistegina lessonii* (40 times maximum exposure time ApoTome-02\_z36c1+2). (b) *SiR-actin* staining of F-actin during the chamber formation in *A. lessonii* (100 times maximum exposure time ApoTome-01\_z13c1+2; Zeiss AxioObserver Z.1 microscope equipped with ApoTome.2). (c) *SiR-actin* staining of F-actin within reticulopodia of *A. lessonii* Zeiss AxioObserver Z.1 microscope equipped with ApoTome.2. (d) *SiR-actin* staining of F-actin within a fragment of reticulopodium in *A. lessonii* Zeiss AxioObserver Z.1 microscope equipped with ApoTome.2



**Figure 9.** SiR-tubulin labeling of granuloreticulopodia in live *Amphistegina lessonii*. DIC/Nomarski merged with epifluorescent ApoTome.2 view. (a) Time lapse 40 times SiR-tubulin DIC washed-ApoTome-01 cut\_t002. (b) Time lapse 20x SiR-tubulin DIC washed-ApoTome-02\_c1+2.

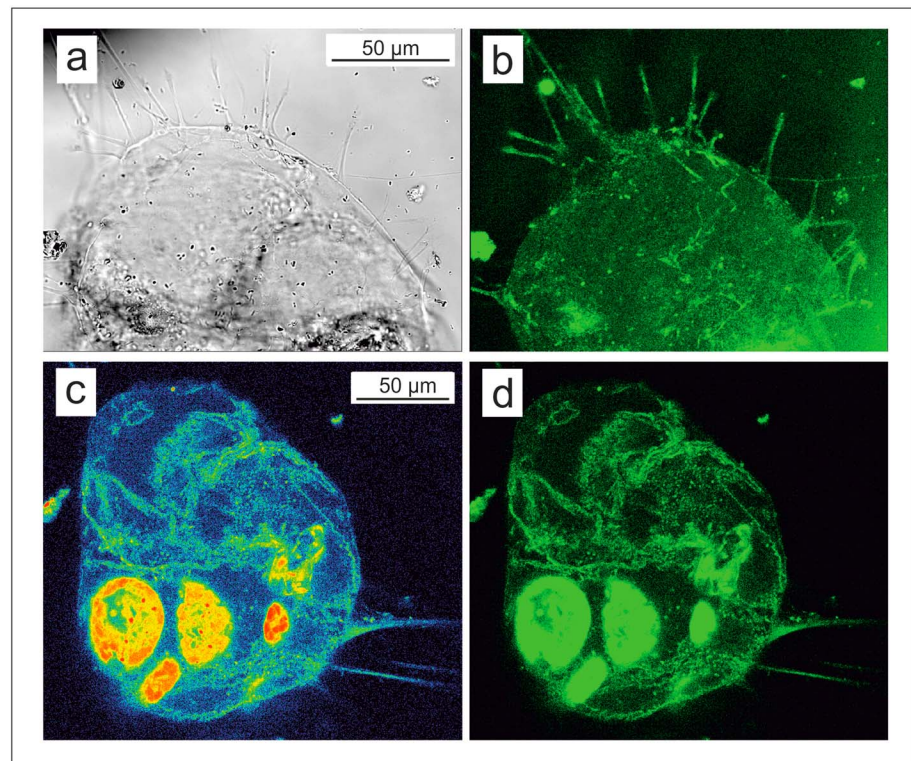
chamber wall. Substantial accumulation of actin is commonly located in the proximity of the new aperture, which opens the test and the last chamber to the external microenvironment (see Tyszka et al., 2019).

SiR-tubulin (Figure 9) labels two types of microstructures in live specimens that either (1) follow elongated branches of pseudopodia or (2) reveal dynamic granules transported along all active pseudopodial structures, including reticulopodia and lamellipodia (in the sense of Travis et al., 1983). (1) Elongated, linear structures are interpreted as thicker bundles of microtubules that construct a cytoskeletal scaffold of reticulopodia (Figure 9), as well as construct “microtubular fibrils” within lamellipodia (see Travis et al., 1983). These labeled structures show a tendency to slow reorganization during continuous transformations of pseudopodia. High resolution observations have not revealed well-labeled single microtubules. (2) The granules labeled with SiR-tubulin are more dynamic than relatively stable elongated fibrillar structures. Their dynamics is expressed by continuous bidirectional motility (Tyszka et al., 2019). Their size and shape may vary from a micrometer to a few micrometers, and from regular equidimensional particles to elongated, often irregular structures always attached to pseudopodia and coated by a plasma membrane.

The *phalloidin* labeling methodology is limited to specimens fixed in methanol-free formaldehyde. Nonetheless, this probe tends to localize the same F-actin microstructures identified by SiR-actin labeling and includes fine actin meshworks, coating most of pseudopodia (such as reticulopodia), as well as all internal surfaces of chambers infilled with the cytoplasm (Figure 10), and chloroplasts. Small granules are also labeled; however, their dynamics cannot be observed. Figures 10a and 10b present *A. lessonii* forming an outer protective envelope (OPE) attached to the substrate (Petri dish glass) during an early stage of chamber formation. Its attachment sites are located at the distal parts of fine and elongated pseudopodial structures that act as “hawsers” stabilizing the foraminiferal test during chamber formation. Such attachment sites at the active phase of OPE formation show the strongest fluorescence due to a higher density of actin meshworks (see Tyszka et al., 2019). This observation follows those of Bowser et al. (1988) and are interpreted as actin-rich plaques involved in adhesion of benthic foraminifera and their reticulopodial structures to substrates. Figures 10c and 10d document another specimen of *A. lessonii* showing a strong autofluorescence signal associated with symbionts (diatoms). Although the *phalloidin* staining procedure shows various limitations (*phalloidin* is highly toxic and lipid membrane impermeable), it is appropriate for double/multiple labeling experiments in order to replace dyes associated with red spectrum fluorescence (e.g., SiR-actin and SiR-based labels).

#### 4.8. Mitochondria

Up to now, mitochondrial structure, distribution, and dynamics were studied on foraminifera through classical approaches, mainly electron microscopy-based methods that do not allow assessment of living cells (Anderson & Lee, 1991). MitoTracker was developed to be used on studies involving qualitative and quantitative parameters of the mitochondria.



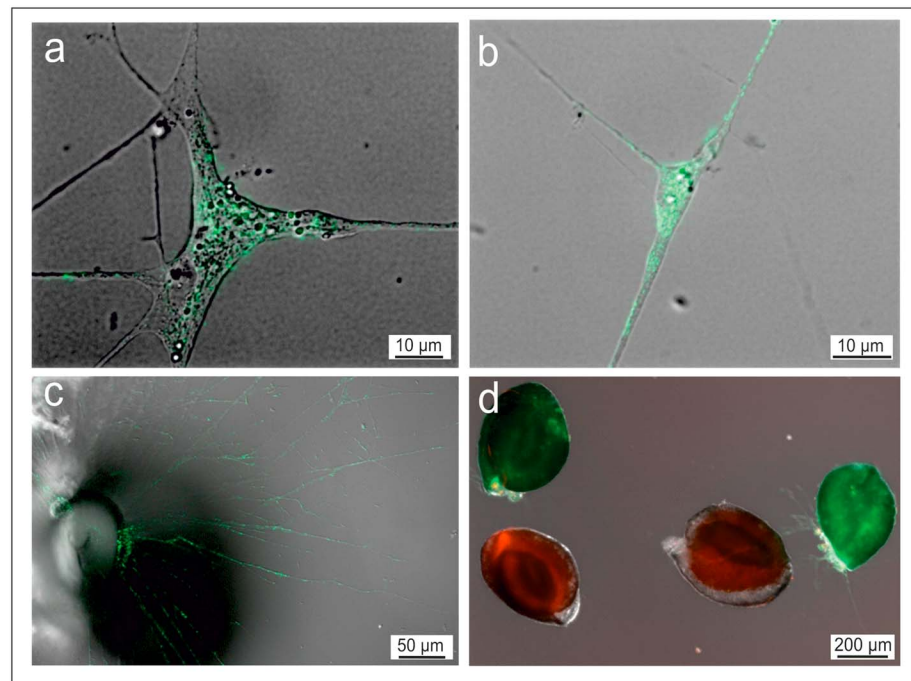
**Figure 10.** *Amphistegina lessonii* fixed and stained with Phalloidin during an early stage of chamber formation. Tests are dissolved in EDTA. (a) Transmission light. (b) Phalloidin staining (green). (c) Phalloidin staining (blue) with a strong signal of autofluorescence from the symbionts (orange/red). (d) Phalloidin staining with autofluorescence (all in green).

MitoTracker® Green FM was tested on specimens of miliolids and *Amphistegina*. Results of these experiments show a sufficient fluorescent signal within most reticulopodial structures (Figures 11a–11c). Additional experiments on pseudopodial structures of *Bolivina variabilis* failed because all individuals retracted reticulopods during incubation. It is supposed that *B. variabilis* is highly sensitive to reagents applied.

Further experiments on miliolids compared staining efficiency of mitochondria within endoplasm vs ectoplasm (reticulopodia). Parallel labeling experiments that applied MitoTracker® Green FM and CellTrace™ Calcein Red-Orange AM were designed to test endoplasmic labeling and validate autofluorescence of miliolid porcelaneous tests. Their results show that both dyes label the cytoplasm within the test (endoplasm) and that their fluorescent signals are more intense than autofluorescence of miliolid porcelaneous tests (Figure 11d). Although MitoTracker® Red FM overlaps with autofluorescence of chlorophyll in symbionts and algal food fragments, clusters of what are presumably mitochondria are evident within lamellipodial structures coating the test (Figure 12).

It should be mentioned that Calcein Red-Orange AM labels intracellular cytoplasm itself, following Calcein Green AM procedure (see Ohno et al., 2016). Its red-orange spectrum allows to avoid the green spectrum and, therefore, limits overlapping signals with different green dyes. It can be applied as an alternative for Calcein Green AM.

CLSM images of specimens incubated in MitoTracker® Red CMXRos showed some well-defined structures within the foraminiferal cell (Figure 13a). Due to their dimensions, these labeled structures are interpreted as algae emitting red autofluorescence. Small red-orange smaller spots are found in the outermost part of the chambers (Figure 13b). The signal is weaker and might possibly represent clusters of mitochondria. Unfortunately, MitoTracker® Red CMXRos appears to not work on the foraminifera examined in this study but additional tests are required.

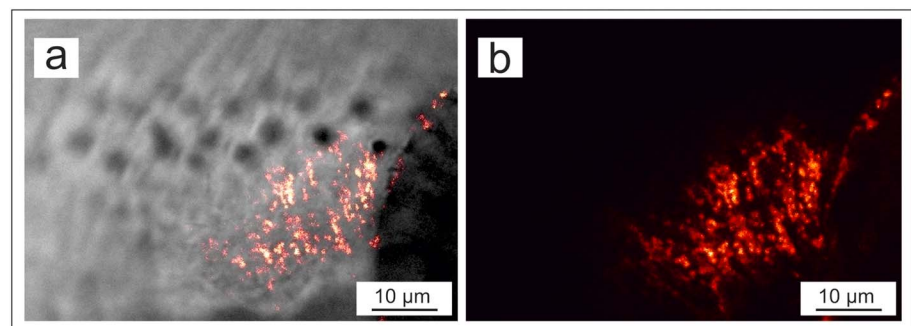


**Figure 11.** (a and b) Details of reticulopodia of *Amphistegina* sp. stained with *MitoTracker*<sup>®</sup> Green FM. (c) Reticulopodia of *Quinqueloculina* sp. stained with *MitoTracker*<sup>®</sup> Green FM. (d) Four specimens of *Quinqueloculina* sp., those in green color were stained with *MitoTracker*<sup>®</sup> Green FM, whereas those in orange were stained with *CellTrace*<sup>™</sup> *Calcein Red-Orange*, AM. Staining was done in two separate Petri dishes; after staining, all specimens were transferred to another Petri dish with clean sea water. Zeiss filter set 63 HE was used for *CellTrace*<sup>™</sup> *Calcein Red-Orange*, AM.

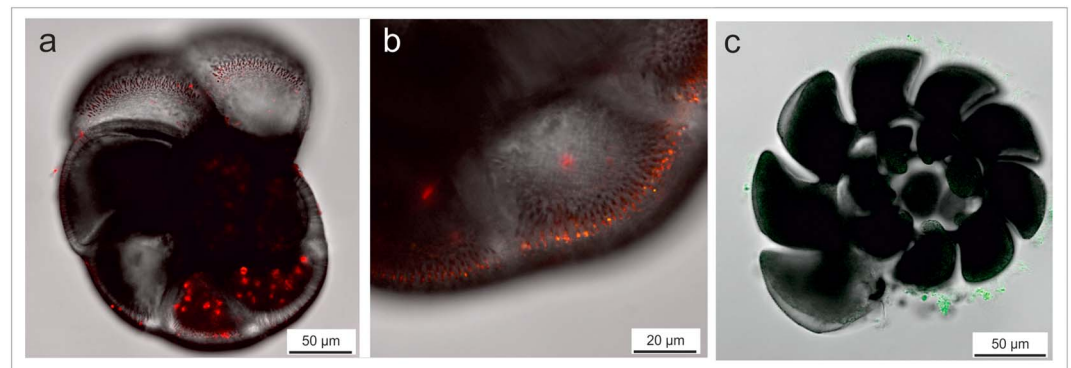
Specimens of *A. tepida* were also used to assess NAO. Despite the application of various protocols (i.e., longer incubations, more concentrated NAO), either NAO did not pass through the cell membrane or mitochondria did not react as expected (Figure 13b). Notwithstanding the unsuccessful test on foraminifera, NAO is a widely used product, having been applied over the last 30 years as a reliable mitochondria marker in different studies such as to assess mitochondrial stress together with *MitoTracker* (Puleston, 2015).

#### 4.9. Nuclei

If the *A. tepida* test was not decalcified, the *NucRed*<sup>™</sup> Live 647 ReadyProbes<sup>™</sup> Reagent did not seem to pass the membrane easily. Only a diffuse but dim far-red emission was observed within the two youngest chambers or in the outer part of the test (not shown). Therefore, an additional probe, *Hoechst 33342* was tested on

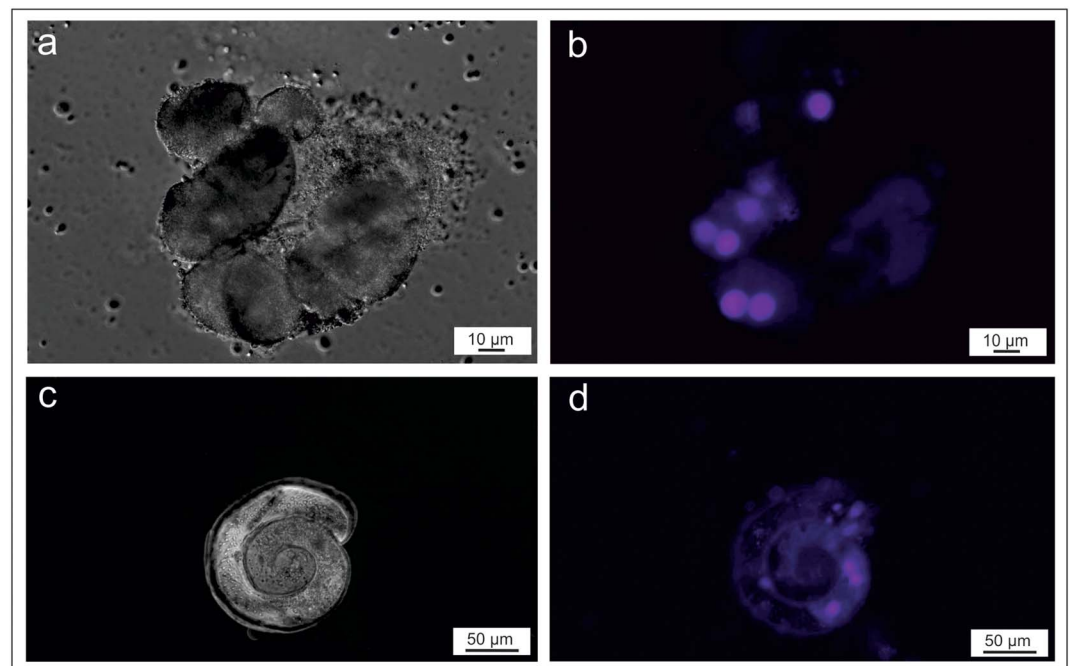


**Figure 12.** *MitoTracker*<sup>®</sup> Red FM live staining of benthic foraminifer *Amphistegina lessonii* d'Orbigny during chamber formation. (a) Stained clusters of mitochondria within lamellipodial structures coating the test (a new chamber and older chambers) during calcification; merged confocal light and transmission light. (b) Confocal light (single fluorescent channel only).

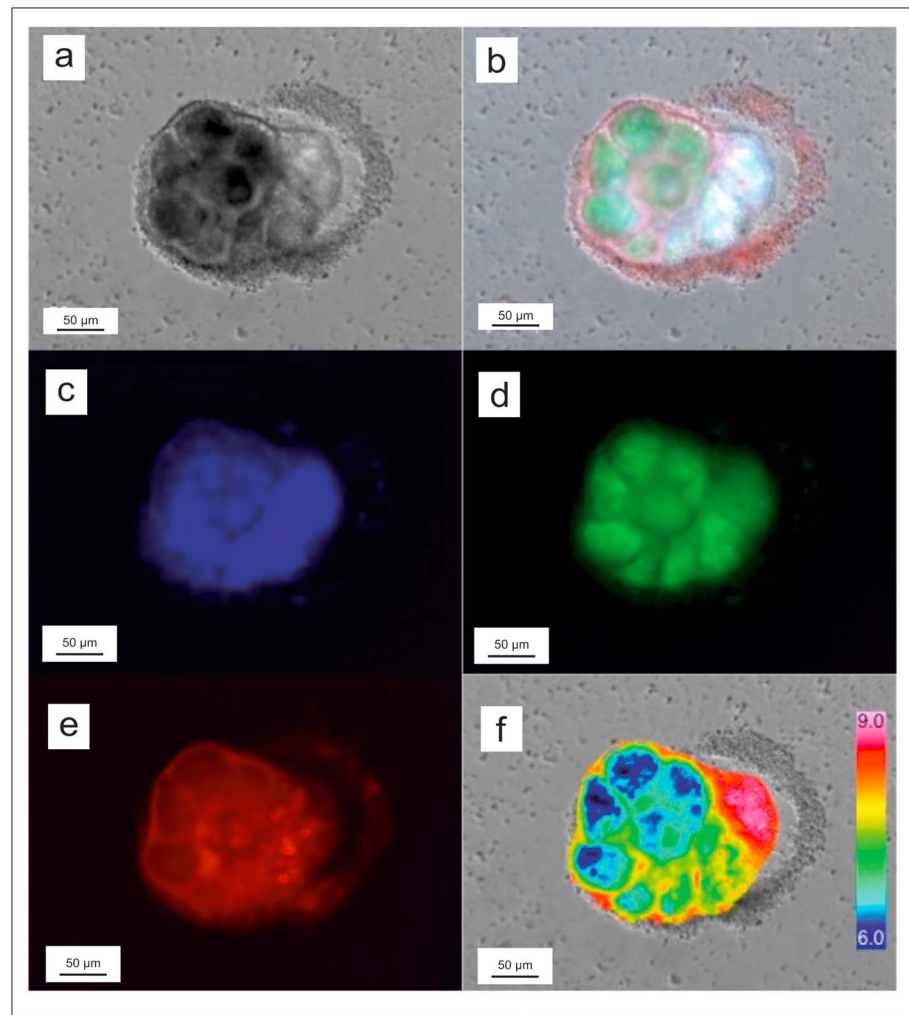


**Figure 13.** Confocal images of foraminifer. (a) *MitoTracker*<sup>®</sup> Red CMXRos with red well-defined fluorescence that are either autofluorescence of algae within the foraminiferal cell or a combination of autofluorescence and *MitoTracker*<sup>®</sup> Red CMXRos labeling. (b) *MitoTracker*<sup>®</sup> Red CMXRos with small red-orange signal in the outermost part of the chamber. (c) *Nonyl Acridine Orange* (NAO) with very low signal as NAO did not pass through the cell membrane.

*Ammonia* sp. and *S. vivipara* (Figure 14). Hoechst 33342 is a nucleic acid protein emitting in blue fluorescence when bound to dsDNA. *Spirillina vivipara* labeled, with a relatively strong fluorescence, without any modification, but *A. beccarii* did not label unless the calcareous test was dissolved. In these species, the fluorescence corresponds to a slightly brighter zone in its Differential Interference Contrast (DIC) image (Figures 14b and 14d) further confirming presence of dsDNA in these locations (i.e., foraminiferal nuclei). Alternatively, these subcellular zones may indicate the presence of DNA of ingested algae or bacteria in phagosomes. The average diameter of the labeled bright spots was approximately 10–25 µm. Commonly several spots were present within one cell and were observed to move through the cell with the protoplasmic streaming (Movie S1). In specimens of *A. beccarii*, the bright spots were even transported from one chamber to another.



**Figure 14.** (a) *Ammonia* sp. individual placed in Ca-free artificial seawater. (b) Localization of nuclei in *Ammonia* sp. after labeling with Hoechst 33342. (c) *Spirillina vivipara*. The test is not decalcified with this species. (d) Localization of nuclei in *S. vivipara* after labeling with Hoechst 33342. Fluorescent signals in the bottom right of Figure 14d correspond with nuclei of food material.



**Figure 15.** Double staining of  $\text{Ca}^{2+}$  and pH with the living calcifying *Ammonia beccarii*. (a) Nomarski microscopy. (b) High-pH (blue), Low-pH (green), and calcium (red) are superimposed on the Nomarski microscopy. (c) High-pH distribution by pyranine (Ex410/Em535). (d) Low-pH distribution by pyranine (Ex470/em535). (e) Ca distribution by Rhod-3AM (Ex550/Em600). (f) Interimage calculation of pH image put on Nomarski microscopy. False color indicates pH variation from 6 (blue) to 9 (red).

another, by passing the narrow aperture between chambers. In both species, the nucleus was not at the periphery. Several nuclei were identified in the observed individuals of both species.

#### 4.10. Foraminiferal Calcification

When a calcareous foraminifer is actively forming a chamber, time series of chemical distributions are particularly interesting. When observing pH ratiometrically, it is necessary to obtain two images using two different filter sets (de Nooijer et al., 2008; de Nooijer, Toyofuku, et al., 2009). Therefore, four sets of images (Nomarski microscopy) are taken as one set for single time slice by taking the set at appropriate time intervals until the end of chamber formation. The cellular pH and Ca distributions within a forming chamber of an *Ammonia* specimen is shown (Figure 15). On the right side of the specimen, a new chamber is formed. In this part, the fluorescence intensity excited by ultraviolet light shows high pH, whereas in other places of the cell, it is excited with blue light and indicates low pH. This result is more easy to interpret when transforming these images into a false-colored one. Calcium signal is also elevated close to the newly formed chamber wall, often seen as an intracellular supply in the form of small accumulations. (Toyofuku et al., 2008).

## 5. Conclusions

Fluorescence imaging in live cells is essential in the understanding of biological processes. We document here the performance and applicability of a wide array of probes to selected calcareous foraminiferal species. These probes were tested to visualize and to label esterase activity, viability, calcium signaling, pH variation, reactive oxygen species, neutral and polar lipids, lipid droplets, cytoskeleton network, Golgi complex, acidic vesicles, nucleus, and mitochondria. It is noteworthy that some probes (BODIPY<sup>TM</sup> TR C5 ceramide, MitoTracker<sup>®</sup> Red CMXRos, NAO, and NucRed<sup>TM</sup> Live 647 ReadyProbes<sup>TM</sup> Reagent) failed even after repeated testing. The application of fluorescence-based methods may be as powerful as transmission electron microscopy.

Indeed, fluorescence techniques allow analysis of living cells, to study organelle distributions and to quantitatively document the number and activity of organelles and their physiology. Furthermore, the application of multiple labels allows assessments of interactions. The choice of probes must, however, be carefully selected based on the target foraminiferal species, requirement for living versus fixed materials, spectroscopic properties of probes (i.e., excitation and emission spectra, quenching, and photobleaching), available equipment and filter set(s), autofluorescence, and probe permeability. In cases of multifluorochrome labeling, separated wavelength emissions, and narrow-emission-spectral-bandwidth probes must be selected to minimize overlap among signals. Fluorescence-based methods into foraminiferal biology may represent, in the future, a complementary or a stand-alone technique with which to study the ultrastructural organization and physiologic processes of the foraminifera.

## Acknowledgments

The authors are very grateful to the Editor-in-Chief Miguel Goni and two anonymous reviewers for their thoughtful and valuable comments that have greatly improved the paper. Markus Raitzsch and Karina Kaczmarek from the AWI, Jakub Kordas from the ZOO Wrocław sp. z o. o. (Poland), and Max Janse from The Royal Burgers' Zoo (Arnhem, the Netherlands) are gratefully acknowledged. The authors declare that no competing interests exist. All the data are included within the paper or the supporting information accompanying it. The research for this paper was partially supported by the Ministero dell'Istruzione, dell'Università e della Ricerca (PRIN 2010-2011 protocollo 2010RMTLYR) to R.C., the Japan Society for the Promotion of Science KAKENHI Grant (Numbers: JP18H06074, JP17H02978, JP19H02009, JP19H03045) to T.T. and Y.N., the WHOI Investment in Science Program to J.M.B., the Polish National Science Center (Grant DEC-2015/19/B/ST10/01944) J.T. and J.G. and the Kuwait Foundation for the Advancement of Sciences (EM084C) to E.A.E.

## References

- Ainsworth, T. D., Hoegh-Guldberg, O., & Leggat, W. (2008). Imaging the fluorescence of marine invertebrates and their associated flora. *Journal of Microscopy*, 232(2), 197–199. <https://doi.org/10.1111/j.1365-2818.2008.02089.x>
- Anderson, O. R., & Lee, J. J. (1991). Cytology and fine structure. In J. J. Lee, & O. R. Anderson (Eds.), *Biology of Foraminifera*, (pp. 335–357). London: Academic Press.
- Armynot du Châtelet, E., & Debenay, J. P. (2010). The anthropogenic impact on the western French coasts as revealed by foraminifera: A review. *Revue de Micropaléontologie*, 53(3), 129–137. <https://doi.org/10.1016/j.revmic.2009.11.002>
- Bentov, S., Brownlee, C., & Erez, J. (2009). The role of seawater endocytosis in the biomineralization process in calcareous foraminifera. *PNAS*, 106(51), 21,500–21,504. <https://doi.org/10.1073/pnas.0906636106>
- Bernhard, J. M. (1988). Postmortem vital staining in benthic foraminifera: Duration and importance in population and distributional studies. *Journal of Foraminiferal Research*, 18(2), 143–146. <https://doi.org/10.2113/gsjfr.18.2.143>
- Bernhard, J. M. (2000). Distinguishing live from dead foraminifera: Methods review and proper applications. *Micropaléontology*, 46(SUPPLEMENT 1), 38–46.
- Bernhard, J. M., Blanks, J. K., Hintz, C. J., & Chandler, G. T. (2004). Use of the fluorescent calcite marker calcein to label foraminiferal tests. *Journal of Foraminiferal Research*, 34(2), 96–101. <https://doi.org/10.2113/0340096>
- Bernhard, J. M., & Bowser, S. S. (1992). Bacterial biofilms as a trophic resource for certain benthic foraminifera. *Marine Ecology Progress Series*, 83, 263–272. <https://doi.org/10.3354/meps083263>
- Bernhard, J. M., & Bowser, S. S. (1996). Novel epifluorescence microscopy method to determine life position of foraminifera in sediments. *Journal of Micropaléontology*, 15(1), 68. <https://doi.org/10.1144/jm.15.1.68>
- Bernhard, J. M., & Bowser, S. S. (1999). Benthic foraminifera of dysoxic sediments: Chloroplast sequestration and functional morphology. *Earth Science Reviews*, 46(1–4), 149–165. [https://doi.org/10.1016/S0012-8252\(99\)00017-3](https://doi.org/10.1016/S0012-8252(99)00017-3)
- Bernhard, J. M., & Bowser, S. S. (2008). Peroxisome proliferation in foraminifera inhabiting the chemocline, An adaptation to reactive oxygen species exposure? *Journal of Eukaryotic Microbiology*, 55(3), 135–144. <https://doi.org/10.1111/j.1550-7408.2008.00318.x>
- Bernhard, J. M., Goldstein, S. T., & Bowser, S. S. (2010). An ectobiont-bearing foraminiferan, *Bolivina pacifica*, that inhabits microoxic pore waters, Cell-biological and paleoceanographic insights. *Environmental Microbiology*, 12(8), 2107–2019.
- Bernhard, J. M., Newkirk, S. G., & Bowser, S. S. (1995). Towards a non-terminal viability assay for foraminiferan protists. *Journal of Eukaryotic Microbiology*, 42(4), 357–367. <https://doi.org/10.1111/j.1550-7408.1995.tb01594.x>
- Bernhard, J. M., Ostermann, D. R., Williams, D. S., & Blanks, J. K. (2006). Comparison of two methods to identify live benthic foraminifera, A test between Rose Bengal and CellTracker Green with implications for stable isotope paleoreconstructions. *Paleoceanography*, 21, PA4210. <https://doi.org/10.1029/2006PA001290>
- Bernhard, J. M., Phalen, W. G., McIntyre-Wressnig, A., Mezzo, F., Wit, J. C., Jeglinski, M., & Filipsson, H. L. (2015). Technical note: Towards resolving in situ, centimeter-scale location and timing of biomineralization in calcareous meiobenthos—The calcein-osmotic pump method. *Biogeosciences*, 12, 5515–5522.
- Borrelli, C., Sabbatini, A., Luna, G. M., Nardelli, M. P., Sbaifi, T., Morigi, C., et al. (2011). Technical note: Determination of the metabolically active fraction of benthic foraminifera by means of Fluorescent In Situ Hybridation (FISH). *Biogeosciences*, 8(8), 2075–2088. <https://doi.org/10.5194/bg-8-2075-2011>
- Bowser, S. S., Travis, J. L., & Rieder, C. L. (1988). Microtubules associate with actin-containing filaments at discrete sites along the ventral surface of *Allogromia* reticulopods. *Journal of Cell Science*, 89, 297–307.
- Braeckman, B., & Raes, H. (1999). The ultrastructural effect and subcellular localization of mercuric chloride and methylmercuric chloride in insect cells (*Aedes albopictus* C6/36). *Tissue & Cell*, 31(2), 223–232.
- Bresler, V., & Yanko, V. (1995a). Acute toxicity of heavy metals for benthic epiphytic foraminifera *Pararotalia spinigera* (Le Calvez) and influence of seaweed-derived DOC. *Environmental Toxicology*, 14(10), 1687–1695. <https://doi.org/10.1002/etc.5620141008>



- Bresler, V., & Yanko, V. (1995b). Chemical ecology. A new approach to the study of living benthic epiphytic foraminifera. *Journal of Foraminiferal Research*, 25(3), 267–279. <https://doi.org/10.2113/gsjfr.25.3.267>
- Chasles, F., Dubertret, B., & Boccara, A. C. (2007). Optimization and characterization of a structured illumination microscope. *Optics Express*, 15(24), 16130–16140. <https://doi.org/10.1364/OE.15.016130>
- Choi, H., Yang, Z., & Weisshaar, J. C. (2015). Single-cell, real-time detection of oxidative stress induced in *Escherichia coli* by the antimicrobial peptide CM15. *Proceedings of the National Academy of Sciences of the United States of America*, 112(3), E303–E310. <https://doi.org/10.1073/pnas.1417703112>
- Chun, H.-S., Jeon, J. H., Pagire, H. S., Lee, J. H., Chung, H.-C., Park, M. J., et al. (2013). Synthesis of LipidGreen2 and its application in lipid and fatty liver imaging. *Molecular BioSystems*, 9(4), 630–633. <https://doi.org/10.1039/c3mb70022d>
- Correia, M. J., & Lee, J. J. (2002). How long do the plastids retained by *Elphidium excavatum* (Terquem) last in their host? *Symbiosis*, 32, 27–38.
- de Freitas Prazeres, M., Martins, S. E., & Bianchini, A. (2011). Biomarkers response to zinc exposure in the symbiont-bearing foraminifera *Amphistegina lessonii* (Amphisteginidae, Foraminifera). *Journal of Experimental Marine Biology and Ecology*, 407(1), 116–121. <https://doi.org/10.1016/j.jembe.2011.07.015>
- de Nooijer, L. J., Langer, G., Nehrke, G., & Bijma, J. (2009). Physiological controls on seawater uptake and calcification in the benthic foraminifer *Ammonia tepida*. *Biogeosciences*, 6(11), 2669–2675. <https://doi.org/10.5194/bg-6-2669-2009>
- de Nooijer, L. J., Reichart, G. J., Dueñas-Bohórquez, A., Wolthers, M., Ernst, S. R., Mason, P. R. D., & van der Zwann, G. J. (2007). Copper incorporation in foraminiferal calcite, Results from culturing experiments. *Biogeosciences*, 4(4), 493–504. <https://doi.org/10.5194/bg-4-493-2007>
- de Nooijer, L. J., Toyofuku, T., & Kitazato, H. (2009). Foraminifera promote calcification by elevating their intracellular pH. *Proceedings of the National Academy of Sciences of the United States of America*, 106(36), 15,374–15,378. <https://doi.org/10.1073/pnas.0904306106>
- de Nooijer, L. J., Toyofuku, T., Oguri, K., Nomaki, H., & Kitazato, H. (2008). Intracellular pH distribution in foraminifera determined by the fluorescent probe HPTS. *Limnology and Oceanography: Methods*, 6(11), 610–618. <https://doi.org/10.4319/lom.2008.6.610>
- Debenay, J. P., Pawlowski, J., & Decrouez, D. (1996). *Les foraminifères actuels*. Paris: Masson.
- Desandier, P.-A., Bonnin, J., Kim, J.-H., Bichon, S., Grémare, A., Deflandre, B., et al. (2015). Lateral and vertical distributions of living benthic foraminifera off the Douro River (western Iberian margin), Impact of the organic matter quality. *Marine Micropaleontology*, 120, 31–45. <https://doi.org/10.1016/j.marmicro.2015.09.002>
- Diaz, G., Melis, M., Batetta, B., Angius, F., & Falchi, A. M. (2008). Hydrophobic characterization of intracellular lipids in situ by Nile Red red/yellow emission ratio. *Micron*, 39(7), 819–824. <https://doi.org/10.1016/j.micron.2008.01.001>
- Dissard, D., Nehrke, G., Reichart, G. J., Nouet, J., & Bijma, J. (2009). Effect of the fluorescent indicator calcein on Mg and Sr incorporation into foraminiferal calcite. *Geochemistry, Geophysics, Geosystems*, 10, Q11001. <https://doi.org/10.1029/2009GC002417>
- Diz, P., Mena, A., Nombela, M. A., Castaño-Carrera, M., Velo, A., Oedóñez, N., et al. (2015). Description of an experimental set up for the culture of benthic foraminifera in controlled pH conditions. *Thalassas*, 31(1), 23–32.
- Evans, D., Müller, W., & Erez, J. (2018). Assessing foraminifera biomineralisation models through trace element data of cultures under variable seawater chemistry. *Geochimica et Cosmochimica Acta*, 236, 198–217. <https://doi.org/10.1016/j.gca.2018.02.048>
- Figueira, B. O., Grenfell, H. R., Hayward, B. H., & Alfaro, A. C. (2012). Comparison of rose Bengal and CellTracker green staining for identification of live salt-marsh foraminifera. *Journal of Foraminiferal Research*, 42(3), 206–215. <https://doi.org/10.2113/gsjfr.42.3.206>
- Frontalini, F., & Coccioni, R. (2008). Benthic foraminifera for heavy metal pollution monitoring: A case study from the central Adriatic Sea coast of Italy. *Estuarine, Coastal and Shelf Science*, 76(2), 404–417. <https://doi.org/10.1016/j.eess.2007.07.024>
- Frontalini, F., & Coccioni, R. (2011). Benthic foraminifera as bioindicators of pollution: A review of Italian research over the last three decades. *Revue de Micropaleontologie*, 54(2), 115–127. <https://doi.org/10.1016/j.revmic.2011.03.001>
- Frontalini, F., Curzi, D., Cesarini, E., Canonico, B., Giordano, F. M., de Matteis, R., et al. (2016). Mercury-pollution induction of intracellular lipid accumulation and lysosomal compartment amplification in the benthic foraminifer *Ammonia parkinsoniana*. *PLoS ONE*, 11(9), e0162401.
- Frontalini, F., Curzi, D., Giordano, F. M., Bernhard, J. M., Falcieri, E., & Coccioni, R. (2015). Effects of lead pollution on *Ammonia parkinsoniana* (foraminifera), Ultrastructural and microanalytical approaches. *European Journal of Histochemistry*, 59, 2460.
- Frontalini, F., Nardelli, M. P., Curzi, D., Martín-González, A., Sabbatini, A., Negri, A., et al. (2018). Benthic foraminiferal ultrastructural alteration induced by heavy metals. *Marine Micropaleontology*, 138, 83–89. <https://doi.org/10.1016/j.marmicro.2017.10.009>
- Gault, C. R., Obeid, L. M., & Hannun, Y. A. (2010). An overview of sphingolipid metabolism, from synthesis to breakdown. *Advances in Experimental Medicine and Biology*, 688, 1–23. [https://doi.org/10.1007/978-1-4419-6741-1\\_1](https://doi.org/10.1007/978-1-4419-6741-1_1)
- Goldstein, S. T. (1999). Foraminifera: A biological overview. In B. K. S. Gupta (Ed.), *Modern foraminifera*, (pp. 37–55). UK: Kluwer Academic Publishers.
- Goldstein, S. T., & Richardson, E. A. (2018). Fine structure of the foraminifer *Haynesina germanica* (Ehrenberg) and its sequestered chloroplasts. *Marine Micropaleontology*, 138, 63–71. <https://doi.org/10.1016/j.marmicro.2017.10.010>
- Goleń, J., Tyszcza, J., Bickmeyer, U., & Bijma, J. (2019). Dynamics and organization of actin-labelled granules as a rapid transport mode of actin cytoskeleton components in Foraminifera. *Biogeosciences Discussions*, 1–25. <https://doi.org/10.5194/bg-2019-182>
- Goulding, J., Abboud, G., Tahilliani, V., Desai, P., Hutchinson, T. E., & Salek-Ardakani, S. (2014). CD8 cells use IFN- $\gamma$  to protect against the lethal effects of a respiratory poxvirus infection. *The Journal of Immunology*, 192(11), 5415–5425. <https://doi.org/10.4049/jimmunol.1400256>
- Greenspan, P., & Fowler, S. D. (1985). Spectrofluorometric studies of the lipid probe, Nile Red. *Journal of Lipid Research*, 26(7), 781–789.
- Greenspan, P., Mayer, E. P., & Fowler, S. D. (1985). Nile red, A selective fluorescent stain for intracellular lipid droplets. *Journal of Cell Biology*, 100(3), 965–973. <https://doi.org/10.1083/jcb.100.3.965>
- Guo, Y., Cordes, K. R., Farese, R. V. Jr., & Walther, T. C. (2009). Lipid droplets at a glance. *Journal of Cell Science*, 122(6), 749–752. <https://doi.org/10.1242/jcs.037630>
- Hintz, C. J., Chandler, G. T., Bernhard, J. M., McCorkle, D. C., Havach, S. M., Blanks, J. K., & Shaw, T. J. (2004). A physicochemically constrained seawater culturing system for production of benthic foraminifera. *Limnology and Oceanography: Methods*, 2(6), 160–170. <https://doi.org/10.4319/lom.2004.2.160>
- Hirose, E. (1999). Pigmentation and acid storage in the tunic, Protective functions of the tunic cells in the tropical ascidian *Phallusia nigra*. *Invertebrate Biology*, 118(4), 414–422. <https://doi.org/10.2307/3227010>
- Jahn, T. L., & Rinaldi, R. A. (1959). Protoplasmic movement in the foraminiferan, *Allogromia laticollaris*, and a theory of its mechanism. *Biological Bulletin*, 117(1), 100–118. <https://doi.org/10.2307/1539042>

- Jauffrais, T., LeKieffre, C., Koho, K. A., Tsuchiya, M., Schweizer, M., Bernhard, J. M., et al. (2018). Ultrastructure and distribution of kleptoplasts in benthic foraminifera from shallow-water (photic) habitats. *Marine Micropaleontology*, *138*, 46–62. <https://doi.org/10.1016/j.marmicro.2017.10.003>
- Jensen, S. S., Peterson, S. A., Halle, B., Aaberg-Jessen, C., & Kristensen, B. W. (2017). Effects of the lysosomal destabilizing drug siramesine on glioblastoma in vitro and in vivo. *BMC Cancer*, *17*(1), 178. <https://doi.org/10.1186/s12885-017-3162-3>
- Johnson, I., & Spence, M. T. Z. (2010). *The molecular probes handbook—A guide to fluorescent probes and labeling technologies*, (11th ed.). Carlsbad, CA: Live Technologies Corporation. ISBN:978-0-9829279-1-5
- Kaczmarzyk, D., Anfelt, J., Särnegrin, A., & Hudson, E. P. (2014). Overexpression of sigma factor SigB improves temperature and butanol tolerance of *Synechocystis* sp. PCC6803. *Journal of Biotechnology*, *182–183*, 54–60.
- Kholmukhamedov, A., Schwartz, J. M., & Lemasters, J. J. (2013). MitoTracker probes and mitochondrial membrane potential. *National Institute of Health*, *39*(6), 543.
- Knight, R., Fauzi, R., & Mantoura, C. (1985). Chlorophyll and carotenoid pigments in Foraminifera and their symbiotic algae, analysis by high performance liquid chromatography. *Marine Ecology Progress Series*, *23*, 241–249. <https://doi.org/10.3354/meps023241>
- Koho, K., LeKieffre, C., Nomaki, H., Salonen, I., Geslin, E., Mabilieu, G., et al. (2018). Changes in ultrastructural features of the foraminifera *Ammonia* spp. in response to anoxic conditions, Field and laboratory observations. *Marine Micropaleontology*, *138*, 72–82. <https://doi.org/10.1016/j.marmicro.2017.10.011>
- Kramar, U., Munsel, D., Berner, Z., Bijma, J., & Nehrke, G. (2010). Determination of trace element incorporation into tests of in vitro grown foraminifera by micro-SYXRF—A basis for the development of paleoproxies. *American Institute of Physics*, *1221*, 154.
- Kurtarkar, S. R., Saraswat, R., Nigam, R., Banerjee, B., Mallick, R., Naik, D. K., & Singh, D. P. (2015). Assessing the effect of calcein incorporation on physiological processes of benthic foraminifera. *Marine Micropaleontology*, *114*, 36–45. <https://doi.org/10.1016/j.marmicro.2014.10.001>
- Langezaal, A. M., Jannik, N. T., Pierson, E. S., & van der Zwann, G. J. (2005). Foraminiferal selectivity towards bacteria, An experimental approach using a cell-permeant stain. *Journal of Sea Research*, *54*(4), 256–275. <https://doi.org/10.1016/j.seares.2005.06.004>
- Le Cadre, V., & Debenay, J. P. (2006). Morphological and cytological responses of *Ammonia* (foraminifera) to copper contamination, Implication for the use of foraminifera as bioindicators of pollution. *Environmental Pollution*, *143*(2), 304–317. <https://doi.org/10.1016/j.envpol.2005.11.033>
- Le Droumaguet, C., Wang, C., & Wang, Q. (2010). Fluorogenic click reaction. *Chemical Society Reviews*, *39*(4), 1233–1239. <https://doi.org/10.1039/B901975H>
- LeKieffre, C., Bernhard, J. M., Mabilieu, G., Filipsson, H. L., Meibom, A., & Geslin, E. (2018). An overview of cellular ultrastructure in benthic foraminifera, New observations in the context of existing literature. *Marine Micropaleontology*, *138*, 12–32. <https://doi.org/10.1016/j.marmicro.2017.10.005>
- Lesser, M. P. (2006). Oxidative stress in marine environments, Biochemistry and physiological ecology. *Annual Review of Physiology*, *68*(1), 253–278. <https://doi.org/10.1146/annurev.physiol.68.040104.110001>
- Lu, S., Sung, T., Lin, N., Abraham, R. T., & Jessen, B. A. (2017). Lysosomal adaptation, How cells respond to lysosomotropic compounds. *PLoS ONE*, *12*(3), e0173771. <https://doi.org/10.1371/journal.pone.0173771>
- Lukinavičius, G., Reymond, L., D'Este, E., Masharina, A., & Göttfert, F. (2014). Fluorogenic probes for live-cell imaging of the cytoskeleton. *Nature Methods*, *11*(7), 731–733. <https://doi.org/10.1038/nmeth.2972>
- Marigómez, I., Soto, M., & Kortabitarte, M. (1996). Tissue-level biomarkers and biological effect of mercury on sentinel slugs, *Arion ater*. *Archives of Environmental Contamination and Toxicology*, *31*(1), 54–62. <https://doi.org/10.1007/BF00203907>
- Martínez, R. A., Isari, S., & Calbet, A. (2014). Use of live, fluorescent-labeled algae for measuring microzooplankton grazing in natural communities. *Journal of Experimental Marine Biology and Ecology*, *457*, 59–70. <https://doi.org/10.1016/j.jembe.2014.03.007>
- McBee, M. E., Chionh, Y. H., Sharaf, M. L., Ho, P., Cai, M. W. L., & Dedon, P. C. (2017). Production of superoxide in bacteria is stress and cell state-dependent, A gating-optimized flow cytometry method that minimizes ROS measurement artifacts with fluorescent dyes. *Frontiers in Microbiology*, *8*, 459.
- Morry, J., Ngamcherdtrakul, W., Gu, S., Goodyear, S. M., Castro, D. J., Reda, M. M., et al. (2015). Dermal delivery of HSP47 siRNA with NOX4-modulating mesoporous silica-based nanoparticles for treating fibrosis. *Biomaterials*, *66*, 41–52. <https://doi.org/10.1016/j.biomaterials.2015.07.005>
- Munsel, D., Kramar, U., Dissard, D., Berner, Z., Bijma, J., Reichart, G.-J., & Neumann, T. (2010). Heavy metal incorporation in foraminiferal calcite, Results from multi-element enrichment culture experiments with *Ammonia tepida*. *Biogeosciences*, *7*(8), 2339–2350. <https://doi.org/10.5194/bg-7-2339-2010>
- Murray, J. W., & Bowser, S. S. (2000). Mortality, protoplasm decay rate, and reliability of staining techniques to recognize “living” foraminifera, A review. *Journal of Foraminiferal Research*, *30*(1), 66–70. <https://doi.org/10.2113/0300066>
- Nardelli, M. P., Barras, C., Metzger, E., Mouret, A., Filipsson, H. L., Jorissen, F. J., & Geslin, E. (2014). Experimental evidence for foraminiferal calcification under anoxia. *Biogeosciences*, *11*(14), 4029–4038. <https://doi.org/10.5194/bg-11-4029-2014>
- Nehrke, G., Keul, N., Langer, G., de Nooijer, L. J., Bijma, J., & Meibom, A. (2013). A new model for biomineralization and trace-element signatures of foraminifera tests. *Biogeosciences*, *10*(10), 6759–6767. <https://doi.org/10.5194/bg-10-6759-2013>
- Nelson, C. D., Spear, R. N., & Andrews, J. H. (2000). Automated image analysis of live/dead staining of the fungus *Aureobasidium pullulans* on microscope slides and leaf surfaces. *BioTechniques*, *29*(4), 874–882. <https://doi.org/10.2144/00294rr04>
- Neumann, M., & Gabel, D. (2002). Simple method for reduction of autofluorescence in fluorescence microscopy. *Journal of Histochemistry and Cytochemistry*, *50*(3), 437–439. <https://doi.org/10.1177/002215540205000315>
- Nomaki, H., Bernhard, J. M., Ishida, A., Tsuchiya, M., Uematsu, K., Tame, A., et al. (2016). Intracellular isotope localization in *Ammonia* sp. (foraminifera) of oxygen-depleted environments, Results of nitrate and sulfate labeling experiments. *Frontiers in Microbiology*, *7*, 163.
- Nomaki, H., LeKieffre, C., Escrig, S., Meibom, A., Yagyu, S., Richardson, E. A., et al. (2018). Innovative TEM-coupled approaches to study foraminiferal cells. *Marine Micropaleontology*, *138*, 90–104. <https://doi.org/10.1016/j.marmicro.2017.10.002>
- Ohno, Y., Fujita, K., Toyofuku, T., & Nakamura, T. (2016). Cytological observations of the large symbiotic foraminifer *Amphisorus kudakajimensis* using calcein acetomethyl ester. *PLoS ONE*, *11*(11), e0165844. <https://doi.org/10.1371/journal.pone.0165844>
- Paoli, L., Guttová, A., Grassi, A., Lackovičová, A., Senko, D., Sorbo, S., et al. (2015). Ecophysiological and ultrastructural effects of dust pollution in lichens exposed around a cement plant (SW Slovakia). *Environmental Science and Pollution Research*, *22*(20), 15,891–15,902. <https://doi.org/10.1007/s11356-015-4807-x>
- Parfley, L. W., & Katz, L. A. (2010). Genome dynamics are influenced by food source in *Allogromia laticollaris* strain CSH (foraminifera). *Genome Biology and Evolution*, *2*(0), 678–685. <https://doi.org/10.1093/gbe/evq051>

- Pawlowski, J., Holzmann, M., & Tyszka, J. (2013). New supraordinal classification of foraminifera, Molecules meet morphology. *Marine Micropaleontology*, *100*, 1–10. <https://doi.org/10.1016/j.marmicro.2013.04.002>
- Petit, J.-M., Maftah, A., Ratinaud, M.-H., & Julien, R. (1992). 10 *N*-Nonyl acridine orange interacts with cardiolipin and allows the quantification of this phospholipid in isolated mitochondria. *European Journal of Biochemistry*, *209*(1), 267–273. <https://doi.org/10.1111/j.1432-1033.1992.tb17285.x>
- Presley, A. D., Fuller, K. M., & Arriaga, E. A. (2003). MitoTracker Green labeling of mitochondrial proteins and their subsequent analysis by capillary electrophoresis with laser-induced fluorescence detection. *Journal of Chromatography B*, *793*(1), 141–150. [https://doi.org/10.1016/S1570-0232\(03\)00371-4](https://doi.org/10.1016/S1570-0232(03)00371-4)
- Pucci, F., Geslin, E., Barras, C., Morigi, C., Sabbatini, A., Negri, A., & Jorissen, F. J. (2009). Survival of benthic foraminifera under hypoxic conditions, Results of an experimental study using the CellTracker Green method. *Marine Pollution Bulletin*, *59*(8–12), 336–351. <https://doi.org/10.1016/j.marpolbul.2009.08.015>
- Puleston, D. (2015). Detection of mitochondrial mass, damage, and reactive oxygen species by flow cytometry. *Cold Spring Harbor Protocols*, *9*, prot086298.
- Rupp, G., Bowser, S. S., Mannella, G. A., & Rieder, C. L. (1986). A naturally occurring tubulin-containing paracrystal in *Allogromia*. *Cell Motility and the Cytoskeleton*, *6*(4), 363–375. <https://doi.org/10.1002/cm.970060403>
- Saben, J., Thakali, K. M., Lindsey, F. E., Zhong, Y., Badger, T. M., Andres, A., & Shankar, K. (2014). Distinct adipogenic differentiation phenotypes of human umbilical cord mesenchymal cells dependent on adipogenic conditions. *Experimental Biology and Medicine*, *239*(10), 1340–1351. <https://doi.org/10.1177/1535370214539225>
- Sackett, D. L., & Wolff, J. (1987). Nile red as a polarity-sensitive fluorescent probe of hydrophobic protein surfaces. *Analytical Biochemistry*, *167*(2), 228–234. [https://doi.org/10.1016/0003-2697\(87\)90157-6](https://doi.org/10.1016/0003-2697(87)90157-6)
- Santulli, C., Brizi, C., Micucci, M., Del Genio, A., De Cristofaro, A., Bracco, F., et al. (2017). *Castanea sativa* Mill. Bark extract protects U-373 MG cells and rat brain slices against ischemia and reperfusion injury. *Journal of Cellular Biochemistry*, *118*(4), 839–850.
- Schliwa, M., & van Blerkom, J. (1981). Structural interaction of cytoskeletal components. *The Journal of Cell Biology*, *90*(1), 222–235. <https://doi.org/10.1083/jcb.90.1.222>
- Schönfeld, J., Alve, E., Geslin, E., Jorissen, F. J., Korsun, S., Spezzaferri, S., & Members of the FOBIMO group (2012). The FOBIMO (Foraminiferal Bio-Monitoring) initiative—Towards a standardized protocol for soft-bottom benthic foraminiferal monitoring studies. *Marine Micropaleontology*, *94–95*, 1–13.
- Schwab, D., & Schlobach, H. (1979). Pigments in monothalamous foraminifera. *Journal of Foraminiferal Research*, *9*(2), 141–146. <https://doi.org/10.2113/gsjfr.9.2.141>
- Shieh, P., Hangauer, M. J., & Bertozzi, C. R. (2012). Fluorogenic azidofluoresceins for biological imaging. *Journal of the American Chemical Society*, *134*(42), 17,428–17,431. <https://doi.org/10.1021/ja308203h>
- Su, L.-C., Hsu, Y.-H., & Wang, H.-Y. (2012). Enhanced labeling of microalgae cellular lipids by application of an electric field generated by alternating current. *Bioresource Technology*, *111*, 323–327. <https://doi.org/10.1016/j.biortech.2012.01.180>
- Takahashi, M., Shibata, M., & Niki, E. (2001). Estimation of lipid peroxidation of live cells using a fluorescent probe, diphenyl-1-pyrenylphosphine. *Free Radical Biology and Medicine*, *31*(2), 164–174. [https://doi.org/10.1016/S0891-5849\(01\)00575-5](https://doi.org/10.1016/S0891-5849(01)00575-5)
- Tesson, B., & Hildebrand, M. (2010). Dynamics of silica cell wall morphogenesis in the diatom *Cyclotella cryptica*, Substructure formation and the role of microfilaments. *Journal of Structural Biology*, *169*(1), 62–74. <https://doi.org/10.1016/j.jsb.2009.08.013>
- Toyofuku, T., de Nooijer, L. J., Yamamoto, H., & Kitazato, H. (2008). Real-time visualization of calcium ion activity in shallow benthic foraminiferal cells using the fluorescent indicator Fluo-3AM. *Geochemistry, Geophysics, Geosystems*, *9*, Q05005. <https://doi.org/10.1029/2007GC001772>
- Toyofuku, T., Matsuo, M. Y., de Nooijer, L. J., Nagai, Y., Kawada, S., Fujita, K., et al. (2017). Proton pumping accompanies calcification in foraminifera. *Nature Communications*, *8*(1), 14145. <https://doi.org/10.1038/ncomms14145>
- Traganos, F., & Darzynkiewicz, Z. (1994). Lysosomal proton pump activity, Supravital cell staining with acridine orange differentiates leukocyte subpopulations. *Methods in Cell Biology*, *41*, 185–194. [https://doi.org/10.1016/S0091-679X\(08\)61717-3](https://doi.org/10.1016/S0091-679X(08)61717-3)
- Travis, J. L., & Allen, R. D. (1981). Studies on the motility of the Foraminifera I. Ultrastructure of the reticulopodial network of *Allogromia laticollaris* (Arnold). *Journal of Cell Biology*, *90*(1), 211–221. <https://doi.org/10.1083/jcb.90.1.211>
- Travis, J. L., & Bowser, S. S. (1986a). A new model of reticulopodial motility and shape, Evidence for a microtubule-based motor and an actin skeleton. *Cell Motility and the Cytoskeleton*, *6*(1), 2–14. <https://doi.org/10.1002/cm.970060103>
- Travis, J. L., & Bowser, S. S. (1986b). Microtubule-dependent reticulopodial motility, Is there a role for actin? *Cell Motility and the Cytoskeleton*, *6*(2), 146–152. <https://doi.org/10.1002/cm.970060212>
- Travis, J. L., & Bowser, S. S. (1988). Optical approaches to the study of foraminiferal motility. *Cell Motility and the Cytoskeleton*, *10*(1–2), 126–136. <https://doi.org/10.1002/cm.970100117>
- Travis, J. L., & Bowser, S. S. (1991). Reticulopodial Motility. In J. J. Lee, & R. O. Anderson (Eds.), *Biology of foraminifera*, (pp. 91–155). London: Academic Press Limited.
- Travis, J. L., Kenealy, J. F., & Allen, R. D. (1983). Studies on the motility of the foraminifera. II. The dynamic microtubular cytoskeleton of the reticulopodial network of *Allogromia laticollaris*. *The Journal of Cell Biology*, *97*(6), 1668–1676. <https://doi.org/10.1083/jcb.97.6.1668>
- Tyszka, J., Bickmeyer, U., Raitzsch, M., Bijma, J., Kaczmarek, K., Mewes, A., et al. (2019). Form and function of F-actin during biomineralization revealed from live experiments on foraminifera. *Proceedings of the National Academy of Sciences of the United States of America*, *116*, 1–6. <https://doi.org/10.1073/pnas.1810394116>
- Van de Meene, A. M. L., & Pickett-Heaps, J. D. (2010). Valve morphogenesis in the centric diatom *Proboscia alata* Sundstrom. *Journal of Phycology*, *38*, 351–363.
- Van Dijk, I., de Nooijer, L. J., & Reichart, G.-J. (2017). Trends in element incorporation in hyaline and porcelaneous foraminifera as a function of pCO<sub>2</sub>. *Biogeosciences*, *14*(3), 497–510. <https://doi.org/10.5194/bg-14-497-2017>
- Van Dijk, I., de Nooijer, L. J., Wolthers, M., & Reichart, G.-J. (2017). Impacts of pH and (CO<sub>3</sub><sup>2-</sup>) on the incorporation of Zn in foraminiferal calcite. *Geochimica et Cosmochimica Acta*, *197*, 263–277. <https://doi.org/10.1016/j.gca.2016.10.031>
- Vasanthi, L. A., Revathi, P., Mini, J., & Munuswamy, N. (2013). Integrated use of histological and ultrastructural biomarkers in *Mugil cephalus* for assessing heavy metal pollution in Ennore estuary, Chennai. *Chemosphere*, *91*(8), 1156–1164. <https://doi.org/10.1016/j.chemosphere.2013.01.021>
- Wang, J., MacEwan, S. R., & Chilkoti, A. (2017). Quantitative mapping of the spatial distribution of nanoparticles in endolysosomes by local pH. *Nano Letters*, *17*(2), 1226–1232. <https://doi.org/10.1021/acs.nanolett.6b05041>
- Williams, D. E., & Hallock, P. (2004). Bleaching in *Amphistegina gibbosa* d'Orbigny (Class Foraminifera), Observations from laboratory experiments using visible and ultraviolet light. *Marine Biology*, *145*(4), 641–649.

- Yanko, V., Arnold, A. J., & Parker, W. C. (1999). Effects of marine pollution on benthic foraminifera. In B. K. Sen Gupta (Ed.), *Modern Foraminifera*, (pp. 217–235). UK: Kluwer Academic Publishers.
- Yorimitsu, T., & Klionsky, D. J. (2005). Autophagy, Molecular machinery for self-eating. *Cell Death and Differentiation*, *12*(S2), 1542–1552. <https://doi.org/10.1038/sj.cdd.4401765>
- Zhao, N., Zhang, A.-S., Worthen, C., Knutson, M. D., & Enns, C. A. (2014). An iron-regulated and glycosylation-dependent proteasomal degradation pathway for the membrane transporter ZIP14. *Proceedings of the National Academy of Sciences of the United States of America*, *111*(25), 9175–9180. <https://doi.org/10.1073/pnas.1405355111>

## References From the Supporting Information

- Allison, N., Austin, H., Austin, W., & Paterson, D. M. (2011). Effects of seawater pH and calcification rate on test Mg/Ca and Sr/Ca in cultured individuals of the benthic, calcitic foraminifera *Elphidium williamsoni*. *Chemical Geology*, *289*(1-2), 171–178. <https://doi.org/10.1016/j.chemgeo.2011.08.001>
- Allison, N., Austin, W., Paterson, D. M., & Austin, H. (2010). Culture studies of the benthic foraminifera *Elphidium williamsoni*: Evaluating pH,  $\Delta$  (CO<sub>2</sub><sup>2-</sup>) and inter-individual effects on test Mg/Ca. *Chemical Geology*, *274*(1-2), 87–93. <https://doi.org/10.1016/j.chemgeo.2010.03.019>
- Barras, C., Duplessy, J.-C., Geslin, E., Michel, E., & Jorissen, F. J. (2010). Calibration of  $\delta^{18}\text{O}$  of cultured benthic foraminiferal calcite as a function of temperature. *Biogeosciences*, *7*(4), 1349–1356. <https://doi.org/10.5194/bg-7-1349-2010>
- Bernhard, J. M., Barry, P., Buck, K. R., & Starczak, V. R. (2009). Impact of intentionally injected carbon dioxide hydrate on deep-sea benthic foraminiferal survival. *Global Change Biology*, *15*(8), 2078–2088. <https://doi.org/10.1111/j.1365-2486.2008.01822.x>
- Cesbron, F., Geslin, E., Jorissen, F. J., Delgard, M. L., Charrieau, L., Deflandre, B., et al. (2016). Vertical distribution and respiration rates of benthic foraminifera, Contribution to aerobic remineralization in intertidal mudflats covered by *Zostera noltei* meadows. *Estuarine, Coastal and Shelf Science*, *179*, 23–38. <https://doi.org/10.1016/j.ecss.2015.12.005>
- Denoyelle, M., Geslin, E., Jorissen, F. J., Cazes, L., & Galgani, F. (2012). Innovative use of foraminifera in ecotoxicology, A marine chronic bioassay for testing potential toxicity of drilling muds. *Ecological Indicators*, *12*(1), 17–25. <https://doi.org/10.1016/j.ecolind.2011.05.011>
- Dissard, D., Nehrke, G., Reichart, G.-J., & Bijma, J. (2010). The impact of salinity on the Mg/Ca and Sr/Ca ratio in the benthic foraminifera *Ammonia tepida*, Results from culture experiments. *Geochimica et Cosmochimica Acta*, *74*(3), 928–940. <https://doi.org/10.1016/j.gca.2009.10.040>
- Dueñas-Bohórquez, A., Raitzsch, M., de Nooijer, L. J., & Reichart, G.-J. (2011). Independent impacts of calcium and carbonate ion concentration on Mg and Sr incorporation in cultured benthic foraminifera. *Marine Micropaleontology*, *81*(3-4), 122–130. <https://doi.org/10.1016/j.marmicro.2011.08.002>
- Filipsson, H. L., Bernhard, J. M., Lincoln, S. A., & McCorkle, D. C. (2010). A culture-based calibration of benthic foraminiferal paleo-temperature proxies,  $\delta^{18}\text{O}$  and Mg/Ca results. *Biogeosciences*, *7*(4), 1335–1347. <https://doi.org/10.5194/bg-7-1335-2010>
- Haynert, K., Schönfeld, J., Riebesell, U., & Polovodova, I. (2011). Biometry and dissolution features of the benthic foraminifera *Ammonia aomoriensis* at high pCO<sub>2</sub>. *Marine Ecology Progress Series*, *432*, 53–67. <https://doi.org/10.3354/meps09138>
- Hayward, B. W., Figueira, B. O., Sabaa, A. T., & Buzas, M. A. (2014). Multi-year life spans of high salt marsh agglutinated foraminifera from New Zealand. *Marine Micropaleontology*, *109*, 54–65. <https://doi.org/10.1016/j.marmicro.2014.03.002>
- Hintz, C. J., Shaw, T. J., Bernhard, J. M., Chandler, G. T., McCorkle, D. C., & Blanks, J. K. (2006). Trace/minor element, Calcium ratios in cultured benthic foraminifera. Part II, Ontogenetic variation. *Geochimica*, *70*(8), 1964–1976. <https://doi.org/10.1016/j.gca.2005.12.019>
- Hintz, C. J., Shaw, T. J., Chandler, G. T., Bernhard, J. M., McCorkle, D. C., & Blanks, J. K. (2006). Trace/minor element, Calcium ratios in cultured benthic foraminifera. Part I, Inter-species and inter-individual variability. *Geochimica*, *70*, 1952–1963.
- Khalifa, G. M., Kirchenbuechler, D., Koifman, N., Kleinerman, O., Talmon, Y., Elbaum, M., et al. (2016). Biomineralization pathways in a foraminifer revealed using a novel correlative cryo-fluorescence-SEM-EDS technique. *Journal of Structural Biology*, *196*, 155–163.
- Langlet, D., Baal, C., Geslin, E., Metzger, E., Zuschin, M., Riedel, B., et al. (2014). Foraminiferal species responses to in situ, experimentally induced anoxia in the Adriatic Sea. *Biogeosciences*, *11*(7), 1775–1797. <https://doi.org/10.5194/bg-11-1775-2014>
- Langlet, D., Geslin, E., Baal, C., Metzger, E., Lejzerowicz, F., Riedel, B., et al. (2013). Foraminiferal survival after long-term in situ experimentally induced anoxia. *Biogeosciences*, *11*, 7463–7480.
- McIntyre-Wressnig, A., Bernhard, J. M., Wit, J. C., & McCorkle, D. C. (2014). Ocean acidification not likely to affect the survival and fitness of two temperate benthic foraminiferal species, Results from culture experiments. *Journal of Foraminiferal Research*, *44*(4), 341–351. <https://doi.org/10.2113/gsjfr.44.4.341>
- Raitzsch, M., Dueñas-Bohórquez, A., Reichart, G.-J., de Nooijer, L. J., & Bickert, T. (2010). Incorporation of Mg and Sr in calcite of cultured benthic foraminifera, Impact of calcium concentration and associated calcite saturation state. *Biogeosciences*, *7*, 869–881.
- Rosenthal, Y., Morley, A., Barras, C., Katz, M. E., Jorissen, F. J., Reichart, G.-J., et al. (2011). Temperature calibration of Mg/Ca ratios in the intermediate water benthic foraminifer *Hyalinea balthica*. *Geochemistry, Geophysics, Geosystems*, *12*, Q04003. <https://doi.org/10.1029/2010GC003333>
- Thibault de Chanvalon, A., Metzger, E., Mouret, A., Cesbron, F., Knoery, J., Rozuel, E., et al. (2015). Two-dimensional distribution of living benthic foraminifera in anoxic sediment layers of an estuarine mudflat (Loire estuary, France). *Biogeosciences*, *12*, 6219–6234.
- Wit, J. C., Davis, M. M., McCorkle, D. C., & Bernhard, J. M. (2016). A short-term survival experiment assessing impacts of ocean acidification and hypoxia on the benthic foraminifer *Globobulimina turgida*. *Journal of Foraminiferal Research*, *46*(1), 25–33. <https://doi.org/10.2113/gsjfr.46.1.25>
- Wit, J. C., de Nooijer, L. J., Barras, C., Jorissen, F. J., & Reichart, G.-J. (2012). A reappraisal of the vital effect in cultured benthic foraminifer *Bulimina marginata* on Mg/Ca values, assessing temperature uncertainty relationships. *Biogeosciences*, *9*, 3693–3704.
- Wollenburg, J. E., Raitzsch, M., & Tiedemann, R. (2015). Novel high-pressure culture experiments on deep-sea benthic foraminifera—Evidence for methane seepage-related  $\delta^{13}\text{C}$  of *Cibicides wuellerstorfi*. *Marine Micropaleontology*, *117*, 47–64. <https://doi.org/10.1016/j.marmicro.2015.04.003>

## Erratum

In the originally published version of this article, the funding information in the Acknowledgments was incomplete. The Acknowledgments have since been corrected, and this version may be considered the authoritative version of record.